M.D. HIDALGO ARAYA

Thesis

"Validation of a single wearable sensor to monitor performance during clinical measures of gait and balance."

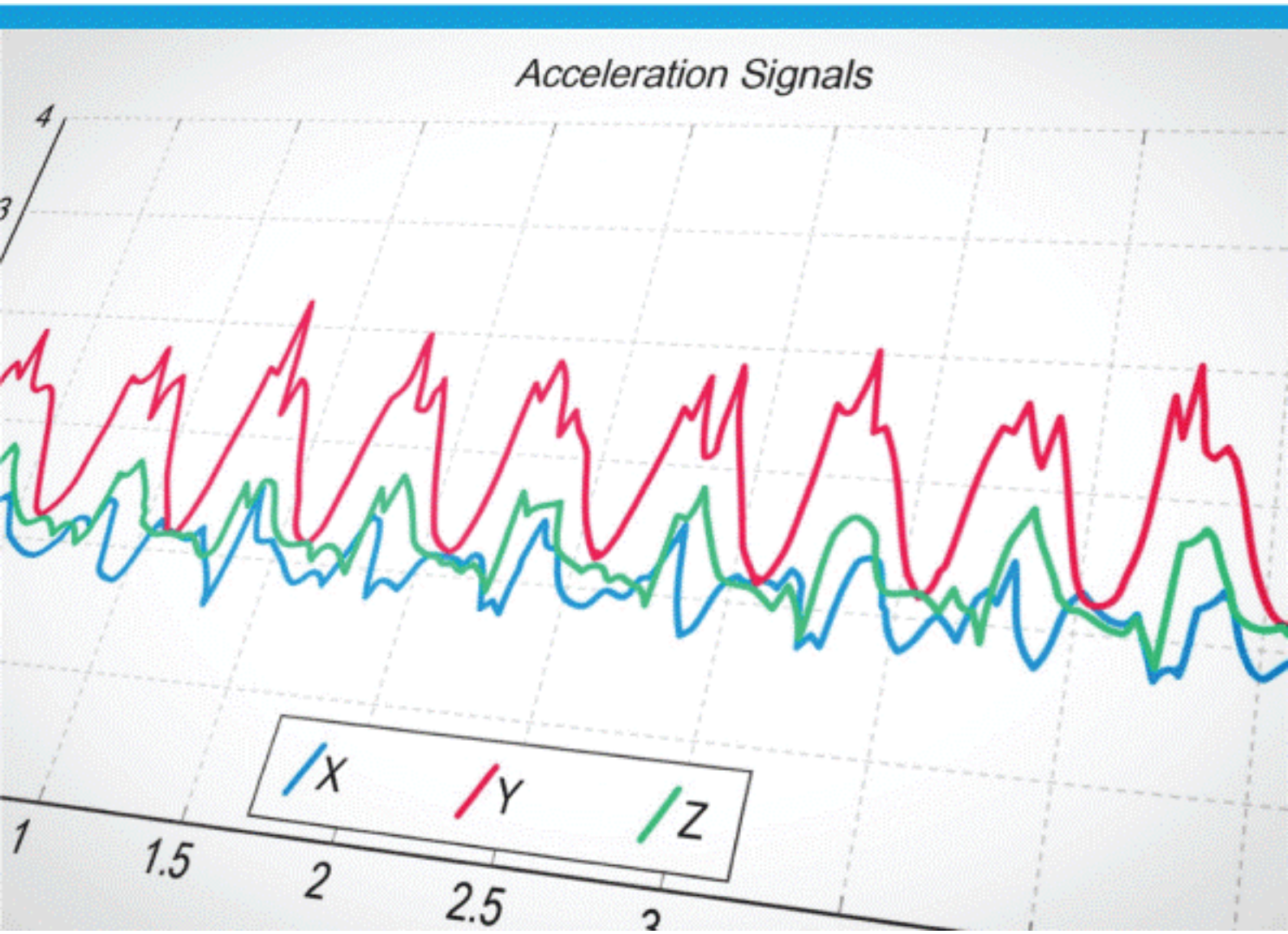

Thesis

"Validation of a single wearable sensor to monitor performance during clinical measures of gait and balance"

By

M.D. Hidalgo Araya

in partial fulfilment of the requirements for the degree of

Master of Science
in Biomedical Engineering
specialization Biomechatronics

at the Delft University of Technology,
to be defended on Wednesday, August 22nd, 2018 at 02:00 PM.

Student:	4602242	
Supervisors:	Prof. Dr. ir. H. Vallery	TU Delft
	A. Jayaraman PT, Ph.D.	Shirley Ryan AbilityLab
	M.K. O'Brien, Ph.D.	Shirley Ryan AbilityLab

TU Delft

This work was supported by the Shirley Ryan AbilityLab (formerly RIC) in Chicago, Illinois, USA.

To my family.

Declaration of Authorship

I hereby confirm that I have authored this Master's thesis independently and without use of sources other than those indicated. All passages which are literally or in a general matter taken out of publications or other sources are marked as such.

Acknowledgments

I would first like to thank my thesis advisor, Professor Dr. ir. H. Vallery at TU Delft, who gave me the opportunity to stay in Chicago to do my thesis. I would also like to thank Dr. Arun Jayaraman, director of the Max Näder Rehabilitation Technologies & Outcomes Lab at the Shirley Ryan AbilityLab and faculty at Northwestern University who without hesitation accepted my application to conduct my second year of studies at his lab. I owe my deepest admiration and gratitude to postdoctoral fellow Dr. M.K. O'Brien at Shirley Ryan AbilityLab for all her guidance, mentorship, endless feedback, support and most importantly welcoming me with open arms. Furthermore, a huge thanks to all the lab members of the CBM Scholars and Rehabilitation Technologies & Outcomes Lab for providing an incredible support network.

Finally, I would like to thank the support of my family, my aunt Vilma who let me stay the whole year at her home in Chicago, and last the endless patience of my girlfriend, who always encourages me to follow my dreams.

List of Abbreviations

10MWT	Ten-meter Walk Test
Acc	Acceleration
AP	Anteroposterior – referring to movement in the sagittal plane
BBS	Berg Balance Scale
CoM	Center of Mass
CWT	Continuous Wavelet Transform
DWT	Discrete Wavelet Transform
EC	End Contact – referring to ending contact of the foot during gait
EMD	Empirical Mode Decomposition
FV	Fast Velocity (condition of the 10MWT)
Gyr	Gyroscope
IC	Initial Contact – referring to initial contact of the foot during gait
ICC	Interclass Correlation
IMF	Intrinsic Mode Function
LA	Level of Approximation
LoA	Limits of Agreement
ML	Mediolateral – referring to movement in the frontal plane
RMS	Root Mean Square
RMSE	Root Mean Square Error
SC	Spectral Centroid
SEC	Standing with Eyes Closed (condition of the BBS)
SFT	Standing with Feet Together (condition of the BBS)
SOL	Standing on One Leg (condition of the BBS)
SSV	Self-Selected Velocity (condition of the 10MWT)
ST	Standing in Tandem stance (condition of the BBS)
SU	Standing Unsupported (condition of the BBS)
SV	Sway Velocity
TUG	Timed Up and Go

Abstract

Deterioration of gait and balance, whether from aging, disease, or injury, has been linked to reduced mobility and increased risk of falling. Wearable sensing technologies, such as inertial measurement units (IMUs), may augment clinical assessments by providing continuous gait and balance data at an increased resolution. The objective of this work was to validate spatiotemporal gait features with a single IMU sensor and to examine changes in sensor-derived features with age during the common clinical tests of gait and balance. We tested the use of an IMU place in the lower back (L5) on age-ranged, healthy individuals (N=34, 20-70 years) during the 10-meter walk test (10MWT), Timed Up and Go (TUG), and Berg Balance Scale (BBS). A total of 49 features were derived from the sensors based on a novel selection of algorithms from previous works. Six spatiotemporal gait features were validated against gold standard measures to assess accuracy and bias. There was an excellent agreement for step time, stance time, swing time, and step count (ICCs 0.90–0.99), and good agreement for gait velocity and step length (ICCs 0.84–0.88). There were 33 linear correlations between age and the sensor-derived features, including a negative correlation between age and vertical displacement of the center of mass during gait. The strongest correlation with age was found for the first slope of the second turn in the TUG ($r=-0.545$, $p\leq0.001$). For the features that showed moderate correlations ($|r|>30$, $p<0.05$), a hierarchical multivariate regression model showed that age was the most important predictor independent of weight, height, and gender. Furthermore, when looking at gender-specific differences after correcting for the contribution of weight and height, women exhibited 5-fold more correlations compared to men. In conclusion, sensor-derived features demonstrated greater sensitivity to individual differences in gait and balance, which may be of a particular interest for future implementation in a clinical setting in impaired populations.

The structure of this thesis is as follows: The first chapter contains the project overview, future vision, and specific aims. The second chapter contains a manuscript that will be submitted for peer-reviewed journal publication. Finally, the third chapter is an appendix with more detailed explanations of the methods and findings of this work.

Contents

List of tables

List of figures

Chapter 1: Project Overview

Stroke affects 15 million people worldwide every year, leaving approximately one-third of this population permanently impaired. In the United States, stroke is considered to be one of the leading cause of long-term disability, affecting more than 795,000 people per year [7]. In Europe, the number of people with stroke was projected to increase by 34% (from 613,000 to 819,771) between 2015-2035 [8]. This causes not only a burden on the individual, family, and community but also on the economy, with hospital care costing an estimated $316.1 billion in the United States between 2012-2013 [7] and 45 billion euros Europe in 2015 [8].

Impairment after stroke varies with the location and level of damage in the brain. The most common outcomes of stroke include the reduced walking speed, hemiparesis, spasticity, impairments in balance, speech, language, and cognition [9, 10]. The primary aim of rehabilitation, medication, and other clinical treatments is to return stroke patients to the highest level of functionality and independent living [11-13]. Therefore, effective and efficient treatment of stroke is particularly important to maximize long-term recovery and minimize economic costs to the patients and hospitals.

Currently, the monitoring, treatment, and evaluation of acute and subacute patients in a stroke unit (i.e. multidisciplinary team of therapy, medical and nursing staff) with gait pathologies rely on infrequent clinical assessments to determine recovery progression. These assessments include performance-based rehabilitation measures as well as subjective and qualitative approaches such as patient self-reports and scoring based on therapist observation [14]. These clinical practices, though effective in maintaining clinical integrity, are not sensitive enough to detect subtle gait changes occurring during the recovery process. Furthermore, these methods suffer for a high inter- and inter-observer variabilities [15], making it difficult to adapt medical and rehabilitation process specific to each patient to maximize recovery. Moreover, these controlled clinical assessments do not necessarily reflect a patient's ability to navigate in more real world settings, such as the home or community. Thus, an objective, reliable, and continuous monitoring system for stroke patients in unconstrained rehabilitation settings would assist clinicians and therapists in making informed decisions about treatment efficacy and recovery progress.

Recent developments in wireless sensing technologies (i.e. accelerometers, gyroscopes, IMUs) have demonstrated an ability to estimate and quantify gait properties without altering the patient's natural movements, leading the transition of the analysis of gait and balance from the constrained laboratory or clinical setting to a naturalistic environment. BioStampRC® (MC10 Inc., USA) is one such wireless and flexible sensor, capable of measuring movement (triaxial accelerometer/gyroscope), electromyography (EMG) and electrocardiography (ECG). These sensors have recently proven effective in measuring relevant clinical outcomes, such as heart rate, muscle activity [16], as well as spatiotemporal gait features [17] and postural sway [18]. However, their usefulness in a clinical setting for continuous monitoring and quantification of impairment has not yet been established.

The long-term goal is to develop a sensor-derived biometric and activity monitoring system that would allow clinicians and therapists to objectively measure post-stroke impairment and recovery both in and out of the hospital (Figure 1). This would enable more personalized, data-driven treatment to improve clinical and functional outcomes. However, before incorporating such a monitoring system, these sensors need to be tested for their feasibility in a clinical environment in healthy controls, which means they need to be checked for their validity (agreement between the value of a measure and the true value), reliability

(reproducibility of the measurement), as well as their ability to quantify measures related to physiological health and mobility. The central hypothesis is that these sensors will be able to capture the clinical and functional outcomes that are currently measured during stroke recovery (i.e. walking speed, balance), and provide additional information about the recovery that is not currently being captured in everyday rehabilitation procedures (i.e. walking asymmetry, postural sway, or turning speed).

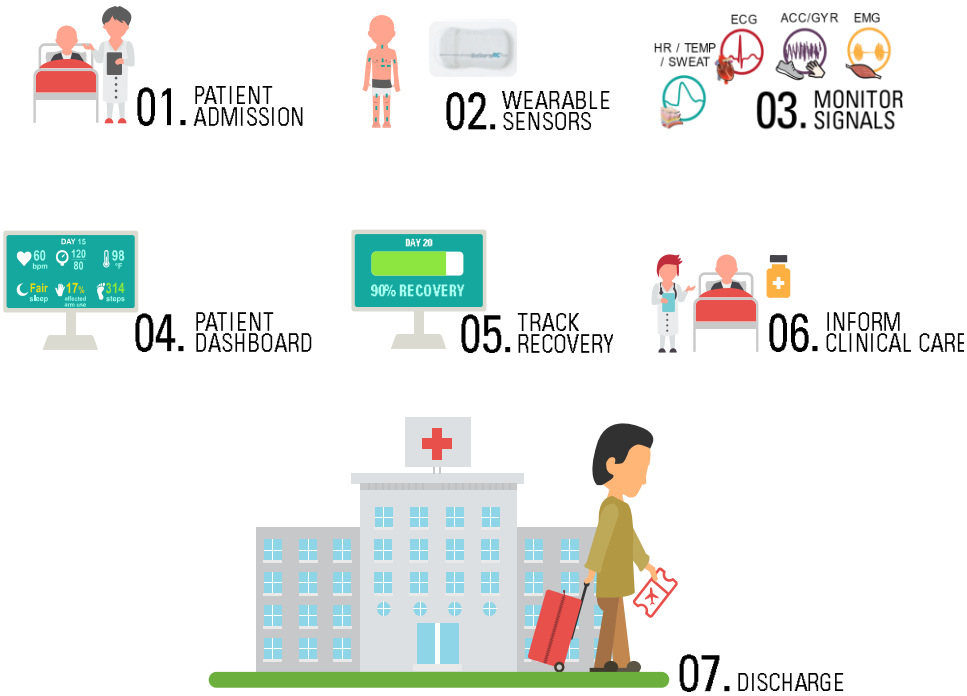

Figure 1. Long term goal and future vision of the project.

This thesis contributes to a larger exploratory clinical trial using these flexible, wearable sensors to monitor stroke recovery. The goal of the thesis work is to test the ability of these sensors to capture clinical and functional data from healthy control individuals, including (i) collecting data from the sensors during common clinical outcome tests of gait and balance, (ii) computing relevant clinical and functional features from sensor data to quantify these clinical outcomes, and (iii) examining changes in these features with age and gender.

The specific aims of the thesis are as follows:

Aim 1. Assess the feasibility of continuous monitoring of healthy adults using wearable sensors

- Obtain quantitative health data from research-grade, wireless, wearable sensors (MC10 BioStampRC®) from age-ranged healthy controls (20-70 years old).
- Validate the BioStampRC® data from the estimated spatiotemporal gait features against different gold standards (i.e. instrumented walkway, visual step count).

Aim 2. Quantify gait, mobility-related activities, and clinical features on healthy individuals.

- Obtain continuous biometric and movement-based sensor data relevant to clinical outcomes (e.g., gait, and static postural balance) during the performance of the following validated clinical tests:
    - 10-Meter Walk Test (10MWT)
    - Timed Up and Go (TUG)
    - Static postural tasks in Berg Balance Scale (BBS)
- Compute additional clinical and movement-derived features during these clinical tests from the device data using previously-validated models. For example, gait asymmetry and static and dynamic balance can be quantified using accelerometer and gyroscope data [2, 19].

Aim 3. Identify changes sensor-derived features with age and gender.

- Apply univariate and multivariate regression techniques to determine how performance changes with age while controlling for weight and height, and to determine the significance of the age as a predictor of these sensor-derived features respectively.
- Compare performance of males and females across the age range.

The expected outcome is to demonstrate the reliability of these wearable sensors to be adopted for a clinical setting and to create of models for movement and balance outcome measures for age-ranged healthy controls, which can later be compared against stroke patients. This will lead to the development of a healthy control database that clinicians can use to monitor disease progression on acute stroke patients, as well as to quantify and predict post-stroke recovery relative to an unimpaired population.

Chapter 2: Manuscript

Title: Augmenting clinical outcome measures of gait and balance with a single inertial sensor in healthy adults.

1. INTRODUCTION

Gait and balance play a vital role in independent functional mobility. From a clinical perspective, these common human activities of everyday living are essential to quantify independent functional mobility and are determinants of quality of life [20], and risk of falls [21] in elderly and impaired populations (i.e. Multiple Sclerosis, Parkinson's Disease). Therefore, clinical outcome measures based on gait and balance can assess and predict how these factors are associated with age-related and phenotype measures.

Currently, clinical outcome measures of walking speed, walking endurance, functional mobility, and static and dynamic balance are used to quantify impairments related to gait and balance. These measures are scored based on both subjective and qualitative assessment, including therapist observation and a single performance metric such as time or distance travelled [14]. Although such measures are effective in maintaining clinical integrity, they are not sensitive enough to detect subtle changes in gait and balance. Additionally, these tests suffer from high inter- and intra-observer variabilities [15], making it difficult to objectively assess patient-specific impairments and improvements in the rehabilitation process.

Wearable sensors, such as inertial measurement units (IMUs), are promising tools to augment the current clinical measures of gait and balance. This technology provides continuous, objective, and high-resolution movement data that may better quantify test performance. Such sensors are also relatively inexpensive, easy to use, lightweight, and unobtrusive when compared with more specialized equipment (i.e. force plates, motion capture systems). These sensors are expected to be reliable tools in assisting clinicians and therapists in making informed decisions about early interventions, treatment efficacy and recovery progress.

BioStampRC (MC10 Inc., USA) is one such flexible, wireless, multimodal, wearable research-grade sensor. We chose this sensor for its low profile and flexible material, as well as for the potential to customize sensing modalities (i.e. pairing accelerometer and gyroscope).

For a realistic implementation of wearable technologies in a clinical setting, one of the constraints is the number of sensors. That is, it is desirable to have the fewest number of sensors possible to quantify performance. The shank and lower back (approximate center of mass) are both relevant locations for gait and balance. Bilateral shank placement of the BioStampRC has previously been validated against an activity monitor [17]. Various algorithms have been developed for a single IMU on the lower back for gait and balance. Using the BioStampRC technology, this single-sensor placement has been validated for balance against force plates [18], but to our knowledge has not been validated in gait. We sought to evaluate the ability of a single BioStampRC sensor on the lower back to quantify both gait and balance in healthy, age-ranged individuals. The authors in [22] explored the changes of gait and balance in age using sensors at multiple locations using the Instrumented Walk Stand and Walk Test (iSAW). However, in order to augment the clinical outcome measures currently used in the current clinical setting we proposed a novel combination of algorithms to extract features across the different clinical tests (i.e. BBS, TUG and 10MWT) used to assess balance, gait and risk of falling with a single sensor placed at the lower back (L5).

The objectives of this study were threefold: (1) validate sensor-derived gait features against gold standard measures to assess accuracy and bias, (2) compute sensor-derived features of gait and balance during common clinical outcome measures for age-ranged healthy individuals, and (3) examine the effect of age and phenotype characteristics (gender, height, weight) on these sensor-derived features. This work lays

a foundation for amassing clinically-relevant baseline features from a healthy population to evaluate recovery progression across different impaired populations (i.e. stroke, multiple sclerosis, etc.).

2. METHODS

2.1. Participants

Thirty-four healthy adults participated in the study (41.3 ± 15 years, range 20 to 70; 20F/14M) and served as a basis for three different age groups (Table 1). Participants had no known musculoskeletal or neurological issues. All individuals provided written informed consent before participation. The study was approved by the Institutional Review Board of Northwestern University (Chicago, IL) in accordance with federal regulations, university policies and ethical standards regarding research on human subjects.

Table 1. Demographic and clinical data of the participants

Age group	*n*	*Mean (SD) age*	*Height (m)*	*Weight (kg)*	*Female*	*Male*
20-34	13	26.2 (3.9)	172.6(11.8)	70.1(13.1)	6	7
35-49	8	38.8 (2.2)	167.6(13.1)	77.5(27.72)	5	3
50-70	13	58.2 (5.8)	168.7(8.6)	72.3(20.3)	9	4

2.2. Protocol and Data Collection

Participants performed a sequence of four tests based on common clinical outcome measures:

- 10-meter walk test (10MWT) of gait speed, with three trials each as a self-selected velocity (SSV) and fast velocity (FV). Increasing gait speed has been correlated with a higher quality of life [20] and community mobility [23]. Participants walked over an instrumented walkway (GAITRite; CIR Systems, Inc.) during this test, which was used as a gold standard for validating spatiotemporal gait features computed from the sensor data.
- Static postural stability items of the Berg Balance Scale (BBS), including: (a) standing unsupported with feet open (SU), (b) standing on one leg (SOL), (c) standing with feet together (SFT), (d) standing in tandem stance (ST), (e) standing with eyes closed (SEC). This test assess functional balance and is associated with risk of falling [21].
- Timed Up and Go (TUG) test of functional mobility, with two trials collected. This test assesses functional mobility and is used to predict the risk of falls [24].
- Participants also performed four self-paced walking bouts in a circuit to validate the step count algorithm. The circuit required straight walking, walking through doorways, and turning corners. Visual step count was used as the gold standard for validating step count computed from sensor data.

2.3. Sensor technology

Participants wore a skin-mounted IMU (BioStampRC; MC10, Inc., dimensions: 65 mm x 35mm x 3 mm, weight: 7g) placed on the fifth lumbar vertebra (L5), approximating the location of the body center of mass (CoM). The sensor was held in place with a transparent adhesive film (Tegaderm; 3M). The BioStampRC was configured to collect tri-axial acceleration (sensitivity ±4g) and tri-axial angular velocity (sensitivity ±2000 deg/s) at 31.25 Hz. Sensor axes were oriented along the anatomical planes: anteroposterior (AP), mediolateral (ML), and vertical (V). A Samsung Galaxy tablet running the proprietary BioStampRC application was used to manage data collect and annotate each clinical test for timestamps (i.e. time when the test started and ended).

De-identified sensor data were uploaded to the MC10 BioStampRC Cloud and then downloaded to a HIPAA-compliant (Health Insurance Portability and Accountability Act of 1996) secure server. Data processing and analysis were implemented in MATLAB 2017a (MathWorks; Natick, MA).

2.4. Excluded participants

Some participants were excluded specifically for some clinical tests: in the 10MWT one participant was excluded due to what appears to be incorrect labelling of the clinical tests. Another participant was excluded only in FV condition because of a particularly fast walking velocity; in this case, the sensor sampling rate was unable to capture the underlying time and frequency components needed to estimate the foot gait events. Finally, two participants were excluded from the TUG analysis because the angular velocity signatures were especially noisy, making it difficult to identify the TUG phases (turning and stand/sit).

2.5. Data analysis

2.5.1. Features Summary

The following features were calculated from the acceleration and angular velocity signals to investigate changes associated with age as summarized in Table 2. Some examples are shown in Figure 4.

Table 2. Estimated features from the clinical tests

Feature	Reference	Units	Definition
BBS			
F50% (AP/ML)	[19, 25]	Hz	Frequencies accounting for 50% of the total power of the signal
F95% (AP/ML)	[19, 25]	Hz	Frequencies accounting for 95% of the total power of the signal
SC (AP/ML)	[19, 25]	Hz	Spectral Centroid. Indication of the center of mass of the spectrum
Max Acc (AP/ML)		m/s^2	Maximum acceleration
Mean Acc (AP/ML)		m/s^2	Mean acceleration
RMS (AP/ML)	[18, 19]	m/s^2	Root mean square of the acceleration
Ellipse Angles (AP,ML)		m/s^2	Angles of 95% of ellipse orientation
95% E. Area	[18, 25]	m^2/s^4	Area of 95% ellipse
Ellipse Axis (AP,ML)	[25]	m/s^2	Length of 95% ellipse axis
Jerk (AP/ML)	[18]	m/s^3	Smoothness of sway. Time derivative of the acceleration
SV (AP/ML)	[18, 19]	m/s	Mean sway velocity
SPathA (ML/AP)	[19]	m/s^2	Total acceleration path
10MWT			
Mean Vertical Displacement		m	Vertical displacement of the Center of Mass (CoM)
Mean Stance Time (SSV/FV)*	[3]	s	Length of time for which the foot is in contact with the ground
Mean Step Time (SSV/FV)*	[3]	s	Length of time for which successive IC of opposite feet
Mean Stride Time(SSV/FV) *	[3]	s	Length of time for which successive IC of the same foot
Mean Swing Time (SSV/FV)*	[3]	s	Length of time for which the foot is not in contact with the ground
Mean Step Length (SSV/FV) *	[3]	cm	Distance of successive IC of opposite feet
Maximum Power Frequency		unitless	Maximum power
Stance Time Symmetry Ratio		unitless	Temporal symmetry ratio between both legs
Step Length Symmetry Ratio		unitless	Spatial symmetry ratio between both legs
Duration (SSV/FV)		s	Time require to complete the test
Mean Velocity (SSV/FV)*	[3]	m/s	Walking velocity averaged over three trials
N Steps (SSV/FV)		unitless	Number of steps taken
Velocity Difference		m/s	Difference in velocity SSV and FV modes
Timed Up and Go			
Sit-to-Stand and Stand-to-Sit			
Range Pitch (i-ii)/(ii-iii)	[26]	deg/s	Difference between the min and max value of the pitch signal
STD Pitch (i-iii)	[26]	deg/s	Standard deviation of the pitch signal
Mean Pitch (i-iii)	[26]	deg/s	Average value of the pitch signal
Median Pitch (i-iii)	[26]	deg/s	Middle value of the pitch signal
Mag Pitch (i-ii)/(ii-iii)	[26]	deg/s	Magnitude value of the pitch signal
Slope Pitch (i-ii)/ (ii-iii)	[26]	deg/s	Rate of change of the pitch signal
Mean Acc AP (i-iii)	[26]	m/s^2	Average phase value of the AP acceleration
STD Acc AP (i-iii)	[26]	m/s^2	Standard deviation of the AP acceleration

Duration (i-iii)	[26]	s	Time require to complete the phase
Median Acc AP (i-iii)	[26]	m/s^2	Middle value of the AP acceleration
Turn 1 and Turn 2			
Duration	[26]	s	Time required to complete the turn phase
N Steps	[26]	unitless	Number of steps taken
Mag Yaw	[26]	deg/s	Magnitude of each turn phase
Slope Yaw (i-ii)/ (ii-iii)	[26]	deg/s	Rate of change of the yaw signal
Walk 1 and Walk 2			
RMS Acc(AP/ML/V)	[26]	m/s^2	Root mean square of the acceleration signal
N Steps	[26]	unitless	Number of steps taken
Mean Step Time	[26]	m/s^2	Average step time over the two walking phases
STD Step Time	[26]	s	Standard deviation of the step time
Walking			
N Steps*		unitless	Number of steps taken

Notes: Acc = acceleration, AP = anteroposterior, ML = mediolateral

2.5.2. Algorithms

Accelerometer signals were transformed to a horizontal-vertical coordinate system [1]. For walking-related clinical tests (10MWT, TUG walking phase, and walking bouts for step count), accelerometer signals were filtered using a second-order zero-lag Butterworth low-pass filter at 10 Hz [3].

1. *Gait Event Detection Algorithm:* Foot contact events were estimated using a continuous wavelet transform approach (CWT) on the preprocessed vertical acceleration a_v [2]. This algorithm uses two wavelets, Gaussian and Mexican Hat, to detect initial contact (IC) and end contact (EC) respectively (*cwt* MATLAB function). To determine the scale for each wavelet, a nonlinear frequency-scale relationship was implemented [4]. First, a_v was integrated and differentiated by CWT using a Gaussian wavelet (*gaus1*), the local minima resulted from the CWT were identified as IC events. The signal was again differentiated using the Mexican Hat wavelet (*gaus2*), and the EC events were identified by the resulted local maxima. Only peaks resulted from the maxima and minima with a magnitude >20% of the mean of all peaks were considered. Upon visual inspection, false IC events were removed by a time interval (0.25-2.25 s) from a previous IC event [5]. Finally, the angular velocity around vertical axis (yaw) was filtered using a fourth-order Butterworth filter at 2 Hz to designate right and left gait events (ICs, ECs) (Figure 2).

   Temporal gait features were estimated by the following equations [3]:

$$\text{Stance Time} = \text{EC}(\text{i}+1) + \text{IC}(\text{i})$$

$$\text{Stride Time} = \text{IC}(\text{i}+2) - \text{IC}(\text{i})$$

$$\text{Step Time} = \text{EC}(\text{i}+1) - \text{IC}(\text{i})$$

$$\text{Swing Time} = \text{Stride Time} - \text{Stance Time}$$

2. *Step Length Estimation Algorithm:* Step length was estimated using a modified inverted pendulum model [6] (Figure 2). During gait the CoM undergoes changes in height, which is used to calculate the step length [27]:

$$\text{Step Length} = 2\sqrt{2\text{lh} - \text{h}^2} + \text{K} \times \text{S}$$

   where l is the pendulum length (sensor location L5 to the ground), h is the change in height obtained by double integration of a_v, S is a vector array of the participants' shoe sizes, and K is a

proportional constant estimated by least squares optimization function [6]. A value of K was determined across participants using:

$$\mathrm{K} = (\mathrm{S^T S})^{-1} \times \mathrm{S^T}(\mathrm{SL_{real,i}} - \text{Step Length})$$

where SL_{real} is a vector array of the true step length obtained from the gold standard (GAITRite) during the 10MWT. Because step length increases with walking speed, two constants were computed for the two velocity conditions: K = 1.32 for SSV and K = 1.70 for FV.

The integration drift of a_v was removed by the Empirical Decomposition Mode (EDM) [6, 28]. First, the vertical velocity v_v is obtained by integrating a_v and then, decomposed into Intrinsic Mode Functions (IMFs), being each IMF component a decomposed waveform of the original v_v going from high-frequency to low-frequency components. In order to select the IMFs to reconstruct v_v without the baseline drift and based on prior visual check the Hurst exponent was implemented as it can serve as a measure of predictability of a time series [29]. Thus, IMFs with Hurst exponent values of < 0.8 were considered. The same process was applied when integrating v_v until obtaining a reconstructed version of the vertical displacement h_v drift-free.

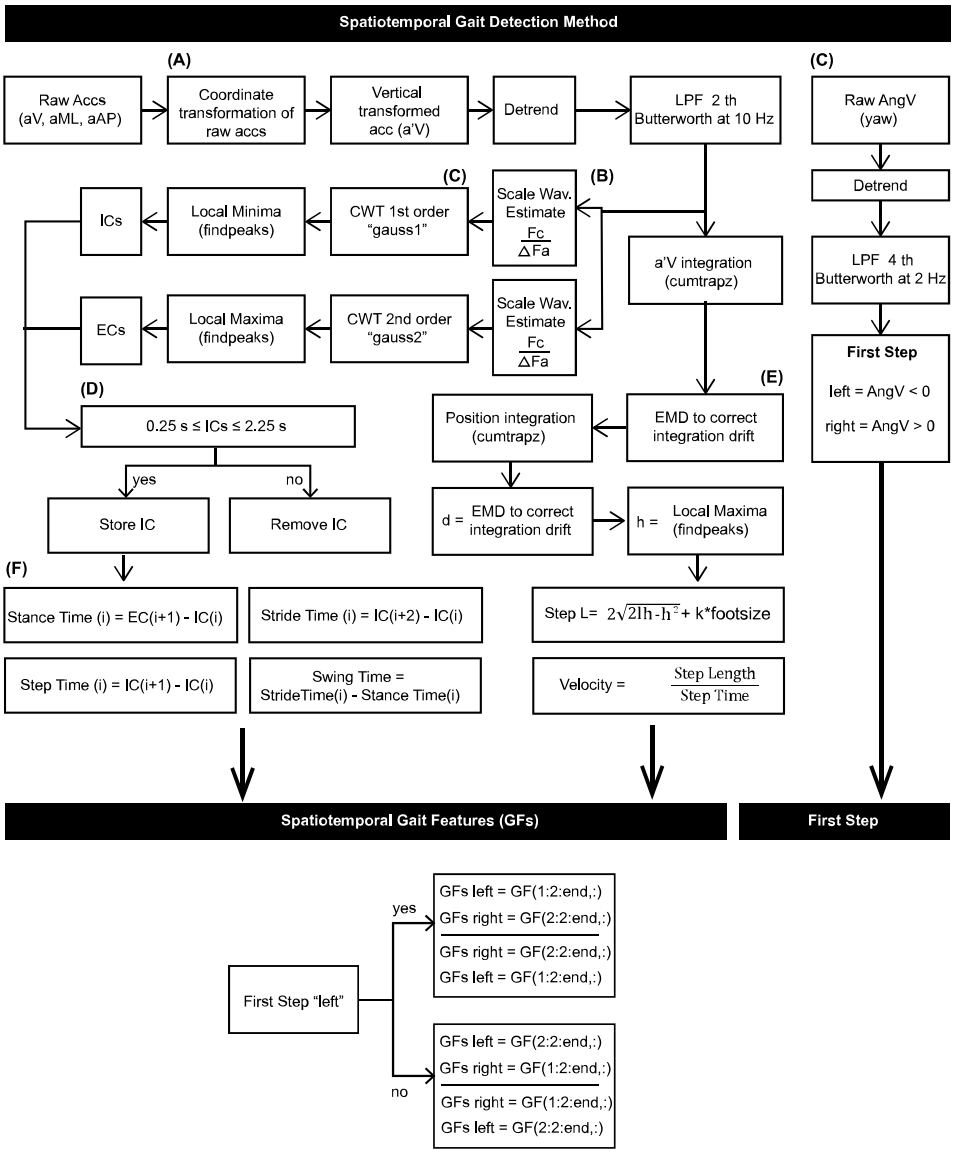

Figure 2. Flowchart to estimate spatiotemporal gait features. Accs = acceleration signals; aV = vertical acceleration, aML = mediolateral acceleration, aAP= anteroposterior acceleration; LPF = low pass filter; Fc = wavelet central frequency; Fa = frequency at the maximum power of the acceleration signal; CWT = continuous wavelet transform; IC= initial contact; EC = end contact; EMD = empirical mode decomposition method; d = vertical displacement; h = vertical displacement peaks; k = optimization constant; AngV = angular velocity; GFs = gait features. A. [1], B.[4], C. [2], D.[5], E.[6], F.[3].

3. *Static Postural Balance Algorithm:* The frequency domain features (Table 2) were estimated from the magnitude of the Fast Fourier Transform (*fft*). Time domain features were estimated by either taking the derivative of the acceleration (Jerk), integration of the acceleration (Mean Velocity), magnitude of the acceleration (RMS). Finally, the ellipse features (Table 2) were obtained by computing the eigen values and vectors of the covariance matrix for the acceleration signals in AP and ML planes [30].

4. *TUG Phase Detection Algorithm:* The algorithm was develop to detect four main phases in the TUG: 1) rising from a chair (sit-to-stand), 2) walking, 3) turning, and 4) sitting down (stand-to-sit) [31-33]. Sit-to-Stand and Stand-to-Sit phases were estimated by a reconstruction of the pitch signal after using a discrete wavelet approach with a Daubechies mother wavelet (db5) and an approximation level 2 (2A). Turning phases were identified under the same approach but using the yaw signal and an approximation level 2 (2A). Finally, to estimate the walking phases and the steps taken in each turn the previously described "Gait Detection Event Algorithm" was used. A flowchart of the algorithm is given in Figure 3.

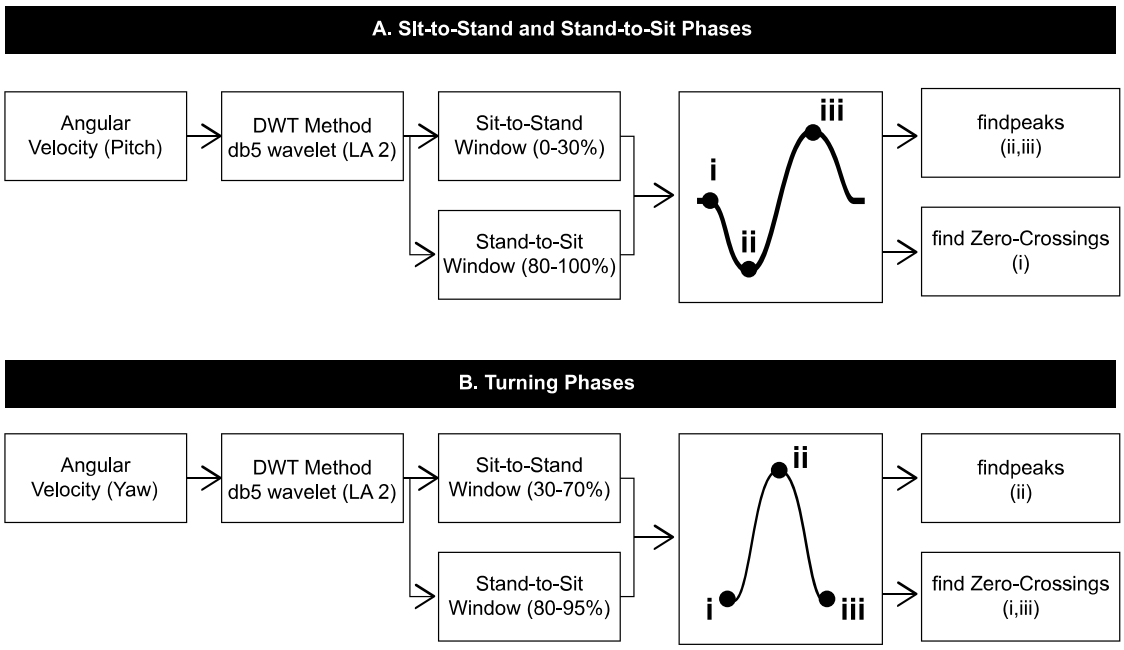

Figure 3. TUG phase detection. A. Sit/stand phases. B. Turning phases. DWT = discrete wavelet transform; db5 = Daubechies 5; LA = level of approximation.

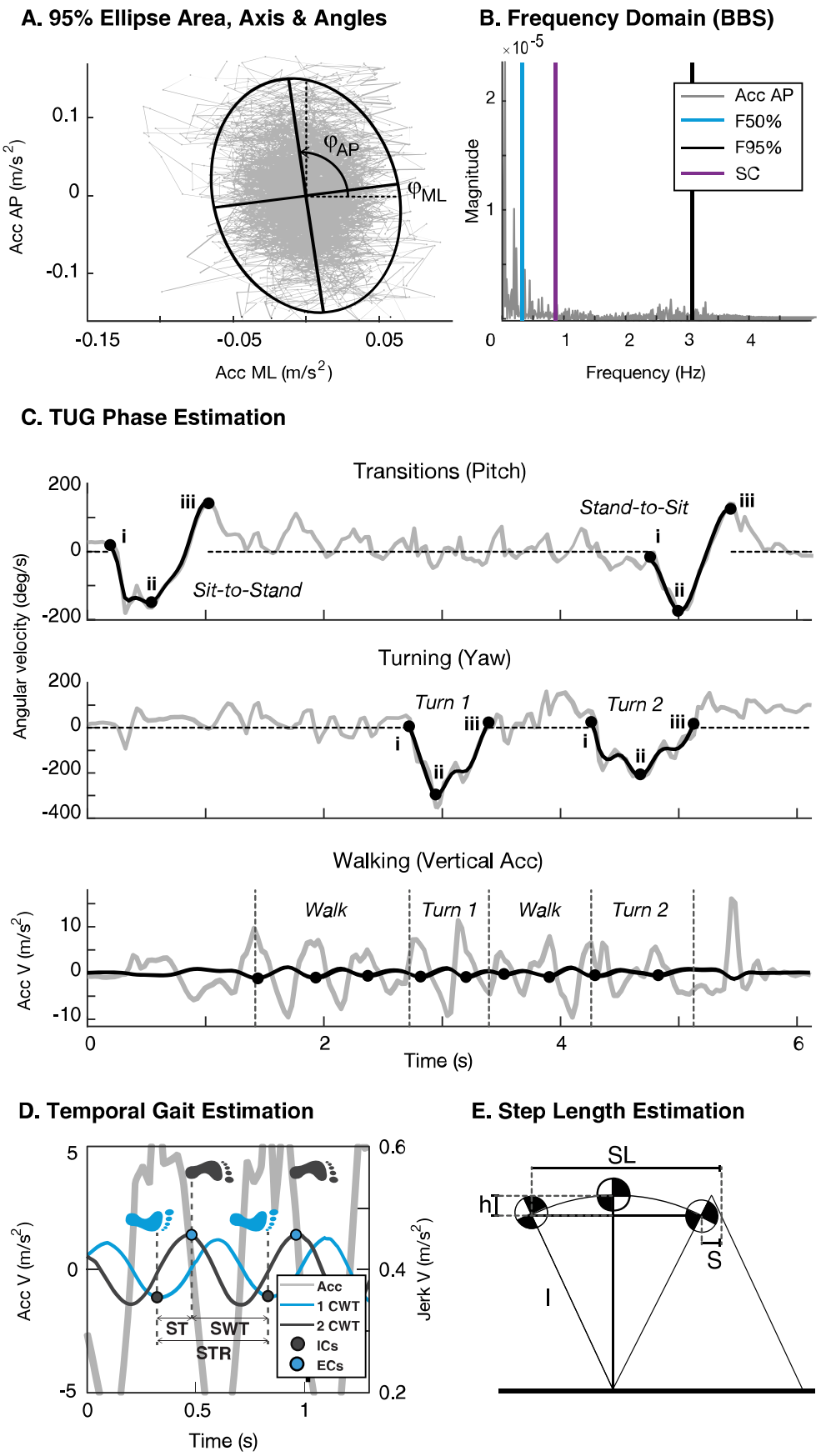

Figure 4. Examples of features estimated from the different clinical tests. (A) 95% Ellipse area, axis and angles. (B). Frequency domain measures from the BBS (F50%, F95% and SC). (C) Phase estimation in the TUG by the DWT method. (D) Temporal gait estimation by the CWT method. (E) Step length estimation by the inverted pendulum model.

2.6. Statistical Analysis

Statistical analysis was done using SPSS v24 (IBM). Bland Altman plots were used to visually check the error distribution between the two systems (i.e. MC10 vs GAITRite; MC10 vs Visual Step Count Etc.). Absolute agreement between the two systems was formally tested using limits of agreement (LoA). Relative agreement between the systems was determine using Pearson's correlation coefficient (r).

Spatiotemporal gait features from both left and right legs were combined, since the healthy controls exhibit relatively symmetrical gait. Gait symmetry was corroborated by computing the empirical cumulative distribution for both left and right in each gait feature.

A total 187 features across all the clinical tests were assessed with univariate analysis for the demographic variables (age, weight, height, and gender). Normality of the features was tested using D'Agustino-Pearson omnibus K^2 with the significance level at 0.05. Feature inter-correlations from one condition of each clinical test were explored using a correlation matrix using the Pearson correlation coefficients [22], to examine the distinction between gait and balance features.

The relationship between each feature and age was assessed using univariate correlations. Strength and direction of the correlations with age were measured with Pearson product-moment correlation for the normally distributed features, and Spearman's rank order correlation for the non-normally distributed features. Furthermore, partial correlations (r*) were performed controlling for the effects of weight and height for all the participants, also separated by gender [22].

Hierarchical multiple regression was performed to quantify the effect of age on features with moderate-to-strong univariate correlations ($|r| > 0.3$ $p < 0.05$). The goal of these models was to determine whether adding age as a predictor variable significantly improves the proportion of explained variance (R^2) for the feature in question. Here, age was added as a predictor variable after adding the variables for weight, height, and gender respectively [22, 34]. These tests for the effect of age alone on a feature after controlling for weight, height, and gender.

Finally, to show the difference and level of resolution of the proposed features versus the current clinical outcome measures (test duration for the TUG, velocity for the 10MWT and therapist scores between 1 and 4 in the BBS), the same clinical outcome measures were tested for differences within clinical tests and between age groups using inferential statistics (two way ANOVAs with main effects of age and test condition, as well as their interaction).

3. RESULTS

3.1. Validation

Figure 5 summarizes the validation results. Bland-Altman plots show mean differences, ICC, and LoA (percentage and upper/lower bounds). Linear correlation plots show p-values for normality (Kolmogorov-Smirnov test), RMSE, and linear equations between BioStampRC and gold standard measurements (GAITRite for spatiotemporal features and manual, visual count for step count estimation)

Excellent agreement was found for the temporal gait features including Step time, Stance time and Swing time (ICC > 0.89, LoA < 15%). Moderate agreement (ICC > 0.84, LoA = 16%) was found for Step Length and velocity.

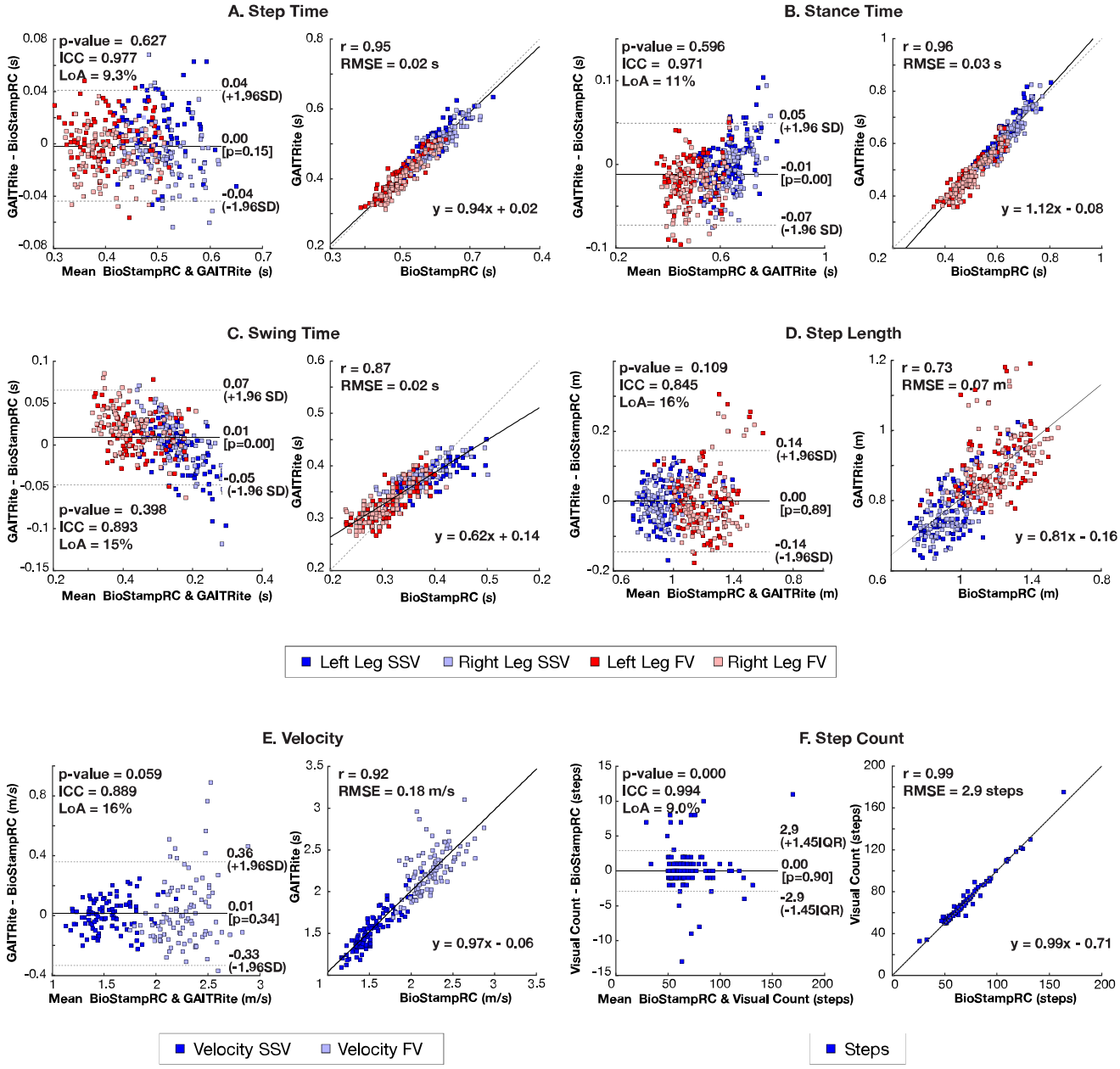

Figure 5. Bland-Altman and linear correlation plots between the BioStampRC and the gold standards for the different spatiotemporal features. RMSE = Root Mean Square Error; ICC = Interclass Correlation; LoA = Limits of Agreement; p-value = Kolmogorov-Smirnov significance value.

3.2. Feature independence between clinical tests

A correlation matrix using Pearson product-moment coefficients (Figure 6) for all the estimated features from one condition of each clinical test illustrates that features were highly correlated within clinical tests but clearly separable between 10MWT and TUG when compared with BBS. This suggests that the features for each clinical test effectively represent different domains. However, there are linear correlations between the 10MWT and TUG, as these tests represent the dynamic domain of mobility (i.e. walking). In the BBS, time and frequency domain features were highly correlated within domains but showed almost no correlation between domains.

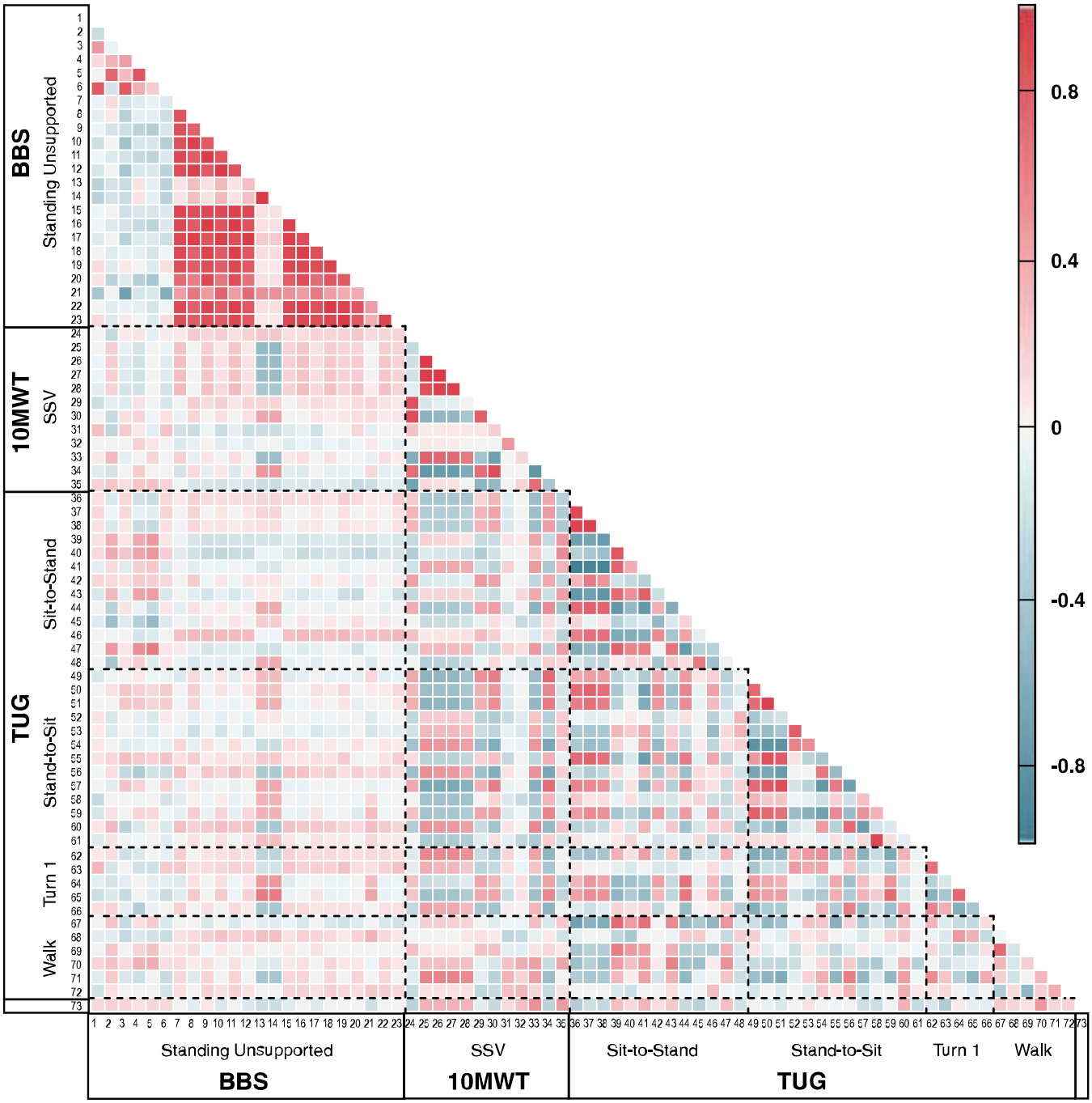

Figure 6. Feature correlation matrix. **BBS Standing Unsupported: 1.** F50% (ML), **2**. F50% (AP), **3**. F95% (ML), **4.** F50% (AP), **5.** SC (AP), **6.** SC (ML), **7.** Max Acc (AP), **8.** Max Acc (ML), **9.** Mean Acc (AP), **10.** Mean Acc (ML), **11.** RMS (AP), **12.** RMS (ML), **13.** Ellipse Angle (AP), **14**. Ellipse Angle (ML). **15.** Ellipse Area, **16.** Ellipse Axis (AP), **17.** Ellipse Axis (ML) **18.** Jerk (AP), **19.** Jerk (ML), **20.** SV (AP), **21.** SV (ML), **22.** SPathA (AP), **23.** SPathA (ML). **10MWT: 24.** Vertical Displacement, **25.** Stance Time, **26.** Step Time, **27**. Stride Time, **28**. Swing Time, **29**. Step Length, **30.** Power Frequency, **31.** Stance Time Ratio, **32.** Step Length Ratio, **33.** Duration, **34.** Mean Velocity, **35.** Step Count. **TUG Sit-to-Stand: 36-37.** Range Pitch (i-ii/ii-iii), **38.** Std Pitch (i-iii), **39.** Mean Pitch (i-iii), **40.** Median Pitch (i-iii), **41-42.** Max Pitch (i-ii/ii-iii), **43-44.** Slope (i-ii/ii-iii), **45.** Mean Acc (AP), **46.** Std Acc (AP), **47.** Duration. **48.** Median Acc (AP). **TUG Stand-to-Sit: 49-50.** Range Pitch (i-ii/ii-iii), **51.** Std Pitch (i-iii), **52.** Mean Pitch (i-iii), **53.** Median Pitch (i-iii), **54-55.** Max Pitch (i-ii/ii-iii), **56-57.** Slope (i-ii/ii-iii), **58.** Mean Acc (AP), **59.** Std Acc (AP), **60.** Duration, **61.** Median Acc (AP). **TUG Turn 1: 62.** Duration, **63.** N Steps, **64.** Mag Yaw, **65-66.** Slope Yaw (i-ii)/ (ii-iii), **TUG Walk: 67-70.** RMS (AP/ML/V), **71.** N Steps, **72.** Mean Step Time, **73.** Std Step Time.

3.3. Correlation between age and sensor-derived features

Tables 4-12 (Appendix below1.A4) show how features across different clinical tests were affected by age. Statistically significant linear correlations with age across the different clinical tests were found in 33 out of 182 features. The strongest correlations with age were found for the TUG in the second turn phase the slope (i-ii) ($r > -0.545$, $p < 0.001$; Table 11, Appendix 1.A4) and for the walking phase the RMS AP ($r > 0.451$ $p<0.001$; Table 11, Appendix 1.A4). Other moderate-to-strong correlations with age ($|r|>0.3$ and $p<0.05$) were found for the BBS: in SEC (2/23 features), F50% (ML) and SC (ML); in SFT (11/23 features), RMS, maximum, mean sway velocity (AP/ML), and mean values of the acceleration (AP/ML), ellipse area, and length of the ellipse axis (AP/ML); in SOL (6/23), the F95% (AP), RMS, maximum, and mean values of the acceleration (ML), mean sway velocity (ML), and length of the acceleration path (ML); in ST (3/23), RMS and mean of the acceleration (AP), and ellipse angle (ML). For the 10MWT FV (1/12), vertical displacement. Finally, for the TUG (11/42), in Sit-to-Stand phase, range of pitch (i-ii), mean pitch (i-iii), magnitude pitch (i-ii) and mean acceleration (AP) (i-iii); in Stand-to Sit phase, range of pitch (i-ii), slope of pitch (ii-iii); in the second turn phase, amplitude of yaw signal (i-ii); finally, in the walking phase, the number of steps.

After adjusting for weight and height, 14 of the 33 features lose their significance. These include: For the BBS, in SEC (1/2 features), SC (ML); in SFT (5/11 features), maximum acceleration (ML), mean acceleration (AP/ML), and mean sway velocity (AP); in SOL (5/6 features), the F95% (AP), RMS, maximum, and mean values of the acceleration (ML), mean sway velocity (ML); in ST (1/2 features), RMS of the acceleration (AP). Finally, for the TUG (2/11 features), in Sit-to-Stand phase, magnitude pitch (i-ii); in walk phase, and the number of steps.

Considering gender differences, women show more statistically significant changes with age than men ($|r|>0.45$ $p<0.05$). Women show significance for 49/187 features, while men show significance for 10/187 features.

Hierarchical multivariate regression analysis for age-effects in sensor-derived features

Table 3 shows the results of the hierarchical multivariate regression for the features that had statistical significant correlations with age > 0.3. Introducing age as a variable in the model significantly increased the amount of explained variance for each feature, by 12.1-26% in 14 out of the 33 features (6/14 in BBS and 8/14 in TUG). From these 14 features, gender was an important predictor for the RMS and mean Acc AP in the SOL balance task; weight and age were important predictors for Range Pitch (i-ii) in the Sit-to-Stand phase, as well as the Slope Pitch (i-ii) in the Stand-to-Sit phase of the TUG. For the rest of the features, age was the only significant predictor.

Table 3. Hierarchical multiple regression analysis from the features that showed moderate-strong correlations with age (|r| > 0.3).

	Features		Standardized Beta Coefficients								
			Weight (kg)	**Height (m)**	**Gender**	**Age (yrs)**	R^2	**Change in R^2**	**F Change**	**df**	**p Value**
10MWT-FV	Vertical Displacement	1	0.260				0.068	0.068	2.172	1/30	0.151
		2	0.046	0.373			0.161	0.093	3.226	1/29	0.083
		3	0.023	0.081	0.366		0.201	0.040	1.410	1/28	0.245
		4	0.067	0.086	0.271	-0.327	0.302	0.101	3.888	1/27	0.059
BBS - SEC	F50% ML	1	-0.117				0.014	0.014	0.429	1/31	0.517
		2	-0.348	0.395			0.116	0.102	3.469	1/30	0.072
		3	-0.331	0.600	-0.258		0.136	0.020	0.0676	1/29	0.418
		4	-0.282	0.621	-0.370	**-0.428**	0.313	0.176	7.187	1/28	**0.012***
	SC ML	1	-0.185				0.034	0.034	1.093	1/31	0.304
		2	-0.358	0.296			0.092	0.057	1.898	1/30	0.179
		3	-0.347	0.426	-0.164		0.100	0.008	0.262	1/29	0.613
		4	-0.308	0.443	-0.255	-0.347	0.216	0.116	4.137	1/28	0.052
BBS - SFT	Max Acc AP	1	-0.235				0.055	0.55	1.809	1/31	0.188
		2	-0.276	0.070			0.058	0.003	0.103	1/30	0.750
		3	-0.248	0.415	-0.433		0.115	0.057	1.852	1/29	0.184
		4	-0.292	0.396	-0.332	**0.386**	0.258	0.143	5.411	1/28	**0.027***
	Max Acc ML	1	-0.050				0.003	0.003	0.078	1/31	0.782
		2	-0.004	-0.092			0.008	0.006	0.169	1/30	0.684
		3	0.032	0.253	-0.434		0.065	0.057	1.765	1/29	0.194
		4	-0.001	0.239	-0.358	0.291	0.146	0.081	2.666	1/28	0.114
	Mean Acc AP	1	-0.264				0.070	0.070	2.322	1/31	0.138
		2	-0.249	-0.025			0.070	0.000	0.013	1/30	0.909
		3	-0.232	0.190	-0.270		0.092	0.022	0.704	1/29	0.408
		4	-0.268	0.175	-0.187	0.317	0.189	0.097	3.344	1/28	0.078
	Mean Acc ML	1	0.047				0.002	0.002	0.070	1/31	0.794
		2	0.050	-0.005			0.002	0.000	0.001	1/30	0.982
		3	0.084	0.402	-0.512		0.081	0.079	2.497	1/29	0.125
		4	0.047	0.387	-0.429	0.316	0.178	0.096	3.274	1/28	0.081
	RMS Acc AP	1	-0.284				0.081	0.081	2.726	1/31	0.109
		2	-0.279	-0.009			0.081	0.000	0.002	1/30	0.969
		3	-0.257	0.265	-0.344		0.117	0.036	1.171	1/29	0.288
		4	-0.299	0.247	-0.247	**0.372**	0.250	0.133	4.961	1/28	**0.034***
	RMS Acc ML	1	0.027				0.001	0.001	0.022	1/31	0.883
		2	0.038	-0.020			0.001	0.000	0.008	1/30	0.930
		3	0.072	0.388	-0.513		0.080	0.079	2.504	1/29	0.124
		4	0.036	0.373	-0.432	0.308	0.172	0.092	3.095	1/28	0.089
	Ellipse L. Axis AP	1	-0.229				0.052	0.052	1.712	1/31	0.200
		2	-0.212	-0.029			0.053	0.001	0.017	1/30	0.896
		3	-0.186	0.290	-0.401		0.101	0.049	1.566	1/29	0.221
		4	-0.228	0.272	-0.304	**0.369**	0.233	0.131	4.796	1/28	**0.037***
	Ellipse L. Axis ML	1	-0.051				0.003	0.003	0.081	1/31	0.778
		2	-0.120	0.118			0.012	0.009	0.275	1/30	0.604
		3	-0.098	0.385	-0.337		0.046	0.034	1.040	1/29	0.316
		4	-0.137	0.369	-0.248	0.339	0.157	0.111	3.675	1/28	0.066
	Ellipse Area	1	-0.208				0.043	0.043	1.407	1/31	0.245
		2	-0.200	-0.014			0.044	0.000	0.004	1/30	0.949
		3	-0.175	0.298	-0.392		0.090	0.046	1.480	1/29	0.234
		4	-0.215	0.281	-0.300	**0.354**	0.211	0.121	4.281	1/28	**0.048***
	SV AP	1	-0.278				0.078	0.078	2.606	1/31	0.117
		2	-0.237	-0.072			0.081	0.003	0.110	1/30	0.743
		3	-0.218	0.157	-0.287		0.106	0.025	0.805	1/29	0.377
		4	-0.253	0.142	-0.206	0.309	0.198	0.092	3.212	1/28	0.084
	SV ML	1	0.168				0.028	0.028	0.896	1/31	0.351
		2	0.190	-0.309			0.029	0.001	0.030	1/30	0.863
		3	0.222	0.347	-0.484		0.100	0.071	2.283	1/29	0.142
		4	0.185	0.331	-0.400	0.323	0.200	0.100	3.512	1/28	0.071
BBS - SOL	F95% AP	1	-0.014				0.000	0.000	0.006	1/31	0.937
		2	-0.063	0.084			0.005	0.005	0.138	1/30	0.713
		3	-0.062	0.098	-0.019		0.005	0.000	0.003	1/29	0.956
		4	-0.100	0.082	0.068	0.333	0.111	0.107	3.356	1/28	0.078

	Max Acc ML	1	-0.177				0.031	0.031	0.998	1/31	0.325
		2	-0.145	-0.053			0.033	0.002	0.058	1/30	0.812
		3	-0.111	0.370	-0.531		0.118	0.085	2.804	1/29	0.105
		4	-0.146	0.355	-0.451	0.305	0.208	0.090	3.176	1/28	0.086
	RMS ML	1	-0.172				0.030	0.030	0.950	1/31	0.337
		2	-0.124	-0.082			0.034	0.004	0.137	1/30	0.714
		3	-0.093	0.304	-0.485		0.105	0.071	2.299	1/29	0.140
		4	-0.125	0.290	-0.412	0.279	0.180	0.075	2.562	1/28	0.121
	SV ML	1	-0.210				0.044	0.044	1.435	1/31	0.240
		2	-0.126	-0.145			0.058	0.014	0.438	1/30	0.513
		3	0.096	0.213	-0.450		0.199	0.061	2.009	1/29	0.167
		4	-0.127	0.200	-0.379	0.270	0.189	0.070	2.432	1/28	0.130
	SPathA ML	1	-0.121				0.015	0.015	0.462	1/31	0.502
		2	-0.095	-0.045			0.016	0.001	0.041	1/30	0.841
		3	-0.082	0.108	-0.193		0.027	0.011	0.335	1/29	0.567
		4	-0.123	0.091	-0.100	0.355	0.149	0.122	3.998	1/28	0.055
BBS - ST	Mean Acc AP	1	0.304				0.093	0.093	3.165	1/31	0.085
		2	0.377	-0.123			0.103	0.010	0.333	1/30	0.568
		3	0.421	0.426	**-0.690**		0.247	0.144	5.540	1/29	**0.026***
		4	0.387	0.412	-0.611	0.303	0.335	0.088	3.723	1/28	0.064
	RMS Acc AP	1	0.349				0.122	0.122	4.303	1/31	0.046
		2	0.392	-0.074			0.125	0.004	0.123	1/30	0.729
		3	0.439	0.502	**-0.724**		0.284	0.158	6.402	1/29	**0.017***
		4	0.409	0.489	-0.653	0.269	0.353	0.070	3.020	1/28	0.093
	Ellipse Angle ML	1	0.035				0.001	0.001	0.038	1/31	0.847
		2	-0.037	0.123			0.011	0.010	0.301	1/30	0.588
		3	-0.054	-0.082	0.258		0.031	0.020	0.600	1/29	0.445
		4	-0.007	-0.062	0.150	**-0.412**	0.195	0.163	5.682	1/28	**0.024***
TUG - Sit-to-Stand	Range Pitch (i-ii)	1	**-0.350**				0.123	0.123	4.193	1/30	**0.049***
		2	-0.428	0.132			0.134	0.011	0.382	1/29	0.541
		3	-0.431	0.091	0.051		0.135	0.001	0.026	1/28	0.873
		4	-0.387	0.109	-0.048	**-0.364**	0.262	0.127	4.656	1/27	**0.040***
	Mean Pitch (i-iii)	1	0.101				0.010	0.010	0.307	1/30	0.583
		2	0.346	-0.418			0.125	0.115	3.801	1/29	0.061
		3	0.355	-0.325	-0.118		0.129	0.004	0.136	1/28	0.715
		4	0.308	-0.344	-0.012	**0.386**	0.272	0.143	5.297	1/27	**0.029***
	Mag Pitch (i-ii)	1	0.334				0.111	0.111	3.755	1/30	0.062
		2	0.416	-0.141			0.124	0.013	0.429	1/29	0.518
		3	0.418	-0.116	-0.032		0.125	0.000	0.010	1/28	0.922
		4	0.377	-0.132	0.062	0.345	0.238	0.114	4.033	1/27	0.055
	Slope Pitch (i-ii)	1	0.021				0.000	0.000	0.013	1/30	0.909
		2	0.186	-0.281			0.052	0.052	1.585	1/29	0.218
		3	0.178	-0.378	0.122		0.057	0.005	0.135	1/28	0.716
		4	0.130	-0.397	0.230	**0.396**	0.207	0.150	5.122	1/27	**0.032***
	Mean Acc AP (i-iii)	1	-0.186				0.035	0.035	1.077	1/30	0.308
		2	-0.197	0.019			0.035	0.000	0.007	1/29	0.933
		3	-0.231	-0.361	0.480		0.105	0.070	2.205	1/28	0.149
		4	-0.189	-0.345	0.387	-0.341	0.217	0.112	3.855	1/27	0.060
TUG - Stand-to-Sit	Range Pitch (i-ii)	1	-0.241				0.058	0.058	1.851	1/30	0.184
		2	-0.141	-0.171			0.077	0.019	0.603	1/29	0.444
		3	-0.131	-0.067	-0.132		0.083	0.005	0.162	1/28	0.690
		4	-0.083	-0.048	-0.241	**-0.400**	0.236	0.154	5.428	1/27	**0.028***
	Slope Pitch (ii-iii)	1	**-0.436**				0.191	0.191	7.060	1/30	**0.013***
		2	-0.321	-0.197			0.216	0.026	0.943	1/29	0.339
		3	-0.317	-0.151	-0.059		0.217	0.001	0.038	1/28	0.847
		4	-0.267	-0.131	-0.171	**-0.412**	0.288	0.163	7.095	1/27	**0.013***
TUG - Turn 2	Amplitude Yaw	1	-0.099				0.010	0.010	0.300	1/30	0.588
		2	-0.086	-0.024			0.010	0.000	0.011	1/29	0.918
		3	-0.085	-0.022	-0.003		0.010	0.000	0.000	1/28	0.994
		4	-0.040	-0.003	-0.106	**-0.380**	0.148	0.138	4.378	1/27	**0.046***
	Slope Yaw (i-ii)	1	-0.113				0.013	0.013	0.390	1/30	0.537
		2	0.022	-0.230			0.048	0.035	1.057	1/29	0.312
		3	0.005	-0.423	0.244		0.066	0.018	0.546	1/28	0.466
		4	0.068	-0.398	0.102	**-0.521**	0.326	0.260	10.427	1/27	**0.003***

TUG - Walk	RMS AP	1	0.215				0.046	0.046	1.460	1/30	0.236
		2	0.286	-0.120			0.056	0.009	0.289	1/29	0.595
		3	0.316	0.228	-0.439		0.115	0.059	1.865	1/28	0.183
		4	0.266	0.208	-0.325	**0.418**	0.282	0.168	6.309	1/27	**0.018***
	N Steps	1	0.018				0.000	0.000	0.010	1/30	0.923
		2	0.039	-0.035			0.001	0.001	0.024	1/29	0.879
		3	0.038	-0.044	0.011		0.001	0.000	0.001	1/28	0.975
		4	-0.006	-0.062	0.111	0.368	0.131	0.130	4.036	1/27	0.055

Notes: Significant standardized beta coefficients are shown in bold.

3.4. Differences within clinical tests and across age groups

An example comparison of the clinical test scores and sensor-derived data is shown in Figure 7 for each test. The 10MWT is scored based on gait velocity. Mean velocities for the SSV and FV conditions were 1.54 ± 0.21 m/s and 2.24 ± 0.23 m/s, respectively (Fig. 7A). There was a main effect of condition on gait velocity ($p<0.001$), but no effect of age group ($p=0.90$). For the sensor-derived feature of vertical displacement of the CoM, mean values in the SSV and FV conditions were 2.3 ± 0.6 cm and 2.5 ± 0.8 cm, respectively (Fig. 7B). In this feature, there was a main effect of age group ($p=0.027$) but not condition ($p=0.132$).

The BBS is scored on a scale of 1 to 4 by a therapist, for an individual's ability to complete a task safely and for the required amount of time. Nearly all participants received a perfect score on the static standing conditions (Fig. 7C), but specific differences between the conditions and age groups is seen in the 95% acceleration ellipse area computed from sensor data (Fig. 7D). Average ellipse areas for each condition were: SU 0.16 ± 0.13 m^2/s^4, SEC 0.06 ± 0.13 m^2/s^4, SFT 0.07 ± 0.06m^2/s^4, SOL 0.41 ± 0.51 m^2/s^4, ST 0.15 ± 0.29 m^2/s^4. There was a main effect of condition ($p<0.001$) but not age group ($p=0.376$) on ellipse area.

Finally, the TUG is scored as a time to complete all five phases of the test. Mean duration of the TUG was 7.41 +/- 1.68 s (Fig. 7E). There was a main effect of age on TUG duration ($p = 0.032$). Post-hoc tests showed that the 20-34 year age group exhibited a shorter duration than the other age groups ($p<0.04$). Our approach can distinguish durations of each phase of the TUG to determine in which phase an individual is moving faster or slower (Fig. 7E, shown as a percentage of the total TUG time). Average durations of each phase were: Sit-to-Stand 0.85 ± 0.20 s, Stand-to-Sit 1.07 ± 0.23 s, first turn 1.44 ± 0.48 s, second turn 1.11 ± 0.33 s, and walk 2.93 ± 0.97 s. There were main effects of phase ($p<0.001$) and age group ($p=0.001$) on phase durations. There were no interaction effects between condition/phase and age for any outcome.

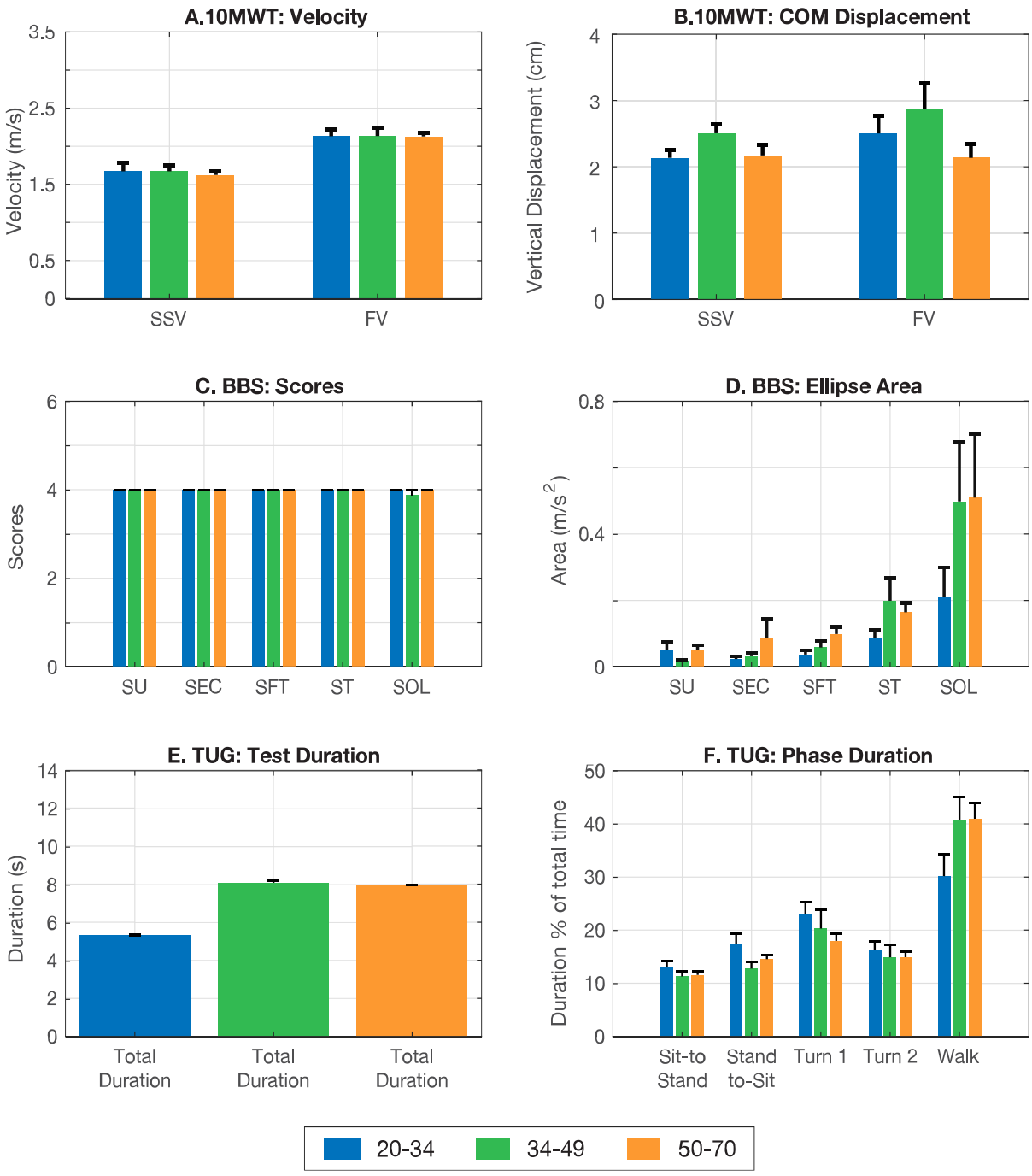

Figure 7. Clinical outcome resolution between the current measures (A, C, E), and the features estimated by the sensor-derived approach (B, D, F) in the different age groups.

4. DISCUSSION

In this study, we estimated features from different clinical outcome tests performed in the rehabilitation setting using a novel combination of algorithms from a single IMU placed at the lower back.

The first objective was to validate sensor-derived gait features against gold standards (GAITRite and visual step count) to explain systematic differences between both systems. Temporal gait features in the 10MWT demonstrated an excellent agreement (mean step time, stance time, and swing time), similar to other studies [2, 3]. Good agreement arose from the step length (ICC = 0.845, LoA = 16%) in which estimation error was proportional to gait velocity (SSV vs. FV condition). A potential explanation for this reduced accuracy in step length is in the walking kinematics. When modelling gait as a rigid inverted pendulum, there is an assumption of an equal exchange between kinetic and gravitational potential energy during walking; that is, increasing gait velocity increases the vertical displacement of the center of mass, and consequentially produces a larger step length [35]. However, most of the participants exhibited only a small change in vertical displacement between the self-selected and fast velocity conditions, which resulted in underestimation of the step length for faster gait velocities. The virtual limb model proposed by [35] may explain such behaviour. In this model, a virtual limb (pendulum) compresses in the stance phase at higher velocities, therefore, reducing vertical displacement of the center of mass, and enhancing elastic energy storage (i.e. in the muscles and tendons). Our findings suggest that elastic energy storage plays an important role for the step length estimation.

The second and third objectives were to compute a series of sensor-derived features during clinical outcome tests of gait, mobility, and balance, and to examine the effect of age and gender on these features. A total of 23 features (time and frequency domain) were estimated for balance in BBS under static standing conditions, 42 features for the estimation of different phases in the TUG, and 13 features to estimate spatiotemporal gait in 10MWT. Of these, 34 features were significantly correlated with age, and women showed 5-fold more age-related correlations compared with men, though this may be explained by the unequal distribution of male and female participants in each age group (Table 1). Hierarchical multivariate regression was employed to determine whether age, gender, height, or weight most contributed to changes in these features. Ultimately, the sensor-derived measures were able to capture more individual differences in clinical outcomes compared with traditional scoring. The findings are discussed below for each clinical outcome test.

Static balance performance in BBS

Our findings confirmed significant decline in balance with aging across the static standing conditions (SU, SEC, SFT, ST, SOL). Following a the pattern reported by [22], participants demonstrated increasing time-domain sway features with age (i.e. mean and maximum velocity, acceleration and jerk) and decreasing frequency domain features in the ML plane (F50% and SC for SEC and F50% for SFT).

Age alone was the most significant predictor of six features in the BBS, including positive correlations with time domain features (Max Acc, RMS, and Ellipse L. Axis in the AP plane, and the Ellipse Area for SFT) and negative correlations with Ellipse Angle in the ML plane for ST and F50% in the ML plane for SEC. The latter showed the strongest relationship with age, meaning older individuals exhibited higher power at lower frequencies. This can be understood as slower postural corrections, which may increase risk of falling. Aging affects neural factors such as increased reaction times [36] and biomechanical factors such as muscle weakness [36], which would affect balance performance in a pattern consistent with our findings.

Finally, we found significant increases in the acceleration ellipse areas across BBS conditions and age groups, which is expected with the increasing difficulty levels of the conditions and aging, since balance is dependent on sensory information and motor abilities.

10MWT performance

A negative correlation in the vertical CoM displacement (maximum peak) for the FV condition was the only significant feature changing with age. This maximum peak occurs in the stance phase, and with aging there is a reduced power during the early stance (hip extension) or late stance (ankle plantarflexion, and hip flexion) phases [37], perhaps due to muscle weakness, which may shorten this vertical displacement.

TUG performance

In line with previous studies, sit-to-stand and stand-to-sit phases in TUG exhibited the strongest correlations with age, related to the angular velocity (pitch signal) [26]. Age alone was the most significant predictor of six features in TUG, including positive correlations with the Mean (i-iii) and Slope (i-ii) of the pitch signal in the sit-to stand phase, as well as RMS Acc AP in the walking phase. We also found negative correlations with Range Pitch (i-ii) in the stand to sit phase, and with magnitude and slope (i-ii) of the yaw signal.

Age and weight together were significant predictors of two features in TUG, with negative correlations with the Range Pitch (i-ii) in the sit-to-stand phase and Slope pitch (ii-iii) in the stand-to-sit phase.

Aging causes lower limb strength deficits (i.e. hip and knee flexion/extension, and ankle dorsiflexion) [38]. Our findings suggest that older individuals rely more on trunk momentum to stand up from a sitting position. Specifically, they exhibit increased flexion of the trunk to translate the CoM to the base of support, and subsequently extend the trunk via increased the angular velocity (pitch) that contributes to the CoM vertical momentum [39, 40]. Finally, the negative correlations in the second turn suggest a slower and more controlled turn before sitting.

Strength and limitations

The strength of this study is in the use of a single sensor to quantify feature associations with age from well-establish clinical outcome tests, different from other studies that used sensors at multiple locations and straightforward tests [22], and validate spatiotemporal gait features with the lowest sampling rate reported in literature to our knowledge. Our study showed that these clinical tests could be grouped into separate domains to assess gait, mobility, and balance. Furthermore, our study expands on the findings in [22], using a different set of features and an implementation in the current clinical outcome tests. Finally, as illustrated in Figure 7, these sensor-derived features can cope with floor/ceiling effects by distinguishing differences between groups and tasks.

There were some limitations to this study. Most notably, this is a small sample size with uneven age distributions between genders. Additional participants across a wider range of ages will be recruited in the future, and a larger sample size with even gender distribution may affect findings.

Future work may also consider incorporating IMUs at the lower limbs to improve the step length estimation, and to maintain accuracy in step detection and spatiotemporal kinematics for gait-impaired populations.

5. CONCLUSION

In summary, we validated the spatiotemporal gait features and quantified age-related changes across well-established clinical outcome tests responsible to quantify gait, mobility, and balance using a single IMU placed at the lower back, we were able to demonstrate that this sensor-derived features can improve the resolution to determine changes related to age, and augment the current clinical outcome measures. Our results suggest that TUG is a reliable test for the quantification of age-related differences. The single sensor approach proved the feasibility and reliability for temporal gait estimation from both left and right legs and not as accurate for the step length estimation using the inverted pendulum.

Overall, this work lays a foundation for amassing clinically-relevant baseline features from a healthy population to evaluate recovery progression across different impaired populations (i.e. stroke, multiple sclerosis, etc.). We expect that this approach would allow clinicians and therapists to better distinguish individual differences when evaluating gait and balance in the laboratory or in the community, thereby paving the way for more data-driven diagnosis and treatment of mobility impairment.

Funding

This work was supported by TU Delft and the Shirley Ryan AbilityLab.

Conflicts of Interest

There was no conflict of interest.

Chapter 3: Appendix

A1 The gait cycle

Bipedal walking is a pseudo-periodic movement (sequence of repeated patterns) called the “gait cycle” that vary within each participant functional and structural locomotor capacity [20]. This task requires the lower limbs for propulsion, while the head, arms and trunk provide stability and balance of the center of mass (CoM). In healthy populations, the gait cycle is characterized by low energy consumption via the exchange of forward kinetic energy and gravitational potential energy of the CoM [41].

There are two main phases of gait: stance and swing. The stance phase comprises approximately the 60% of the gait cycle while the remaining 40% is the swing phase. However, when analyzing pathological gaits (i.e. people with stroke) additional phases are identified to detect subtle changes in the gait pattern, giving more information on the specific gait pathology. For instance, [20] proposed a classification divided into nine phases: initial, loading response, mid stance, terminal stance, pre swing, end contact, initial swing, mid swing and terminal swing (Figure 8).

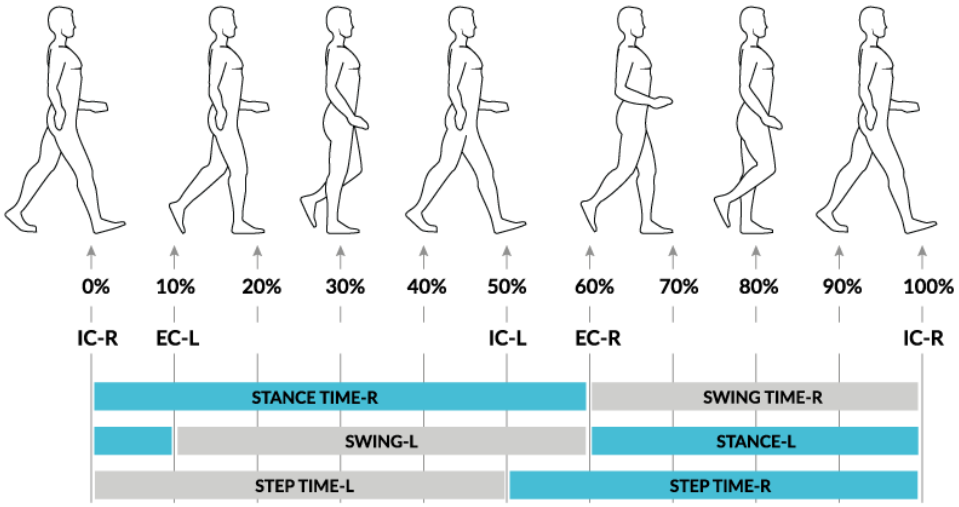

Figure 8. Different gait phases.

- **Initial Contact (IC):** Time when the foot initially starts the contacts with the ground. In healthy people, this typically corresponds to heel strike.

- **Loading Response (LR):** Transition phase between double support and single support. In other words, this phase is the time from when the foot is in contact with the floor until the contralateral foot is prepared to begin its swing phase. The body decelerates when the foot completely lands in the ground, which is achieved by energy absorption mainly at the knee and hip. This phase accounts for approximately 10% of the gait cycle.

- **Mid-Stance (MS):** Begins when contralateral foot starts to swing and finishes when the CoM is aligned over the forefoot. Here, the knee and hip are extended while the ankle is dorsiflexed to align the weight. This phase accounts for approximately 25% of the gait cycle.

- **Terminal Stance (TS):** End of the single limb support, spanning from the time when the heel of the supporting leg is rising until the contralateral foot achieves IC. In the process, the CoM moves away from the base of support. This phase accounts for approximately 20% of the gait cycle.

- **Pre-Swing (PS):** Final phase of the double stance interval. Begins with IC of the contralateral foot until the end contact (EC) the foot. This phase accounts for approximately 10% of the gait cycle.

- **End Contact (EC):** Time when the foot ends contact with the ground, also known as toe-off.

- **Initial Swing (IS):** Foot leaves the ground in order to advance the knee and flex the hip.

- **Mid-Swing (MS):** During mid-swing, the foot clearance is mainly achieved through ankle dorsiflexion. The knee extends in response to the inertia.

- **Terminal Swing (TS):** Final part of swing phase, which ends when the foot achieves contact with the ground (IC).

A2 Clinical outcome measures implemented in the study protocol

The clinical outcome measures used in this protocol were taken from the Shirley Ryan AbilityLab Rehabilitation Measures Database [42]:

A3.1 Berg Balance Scale (BBS)

This test examines dynamic balance (anticipatory postural adjustments, reactive postural control, sensory orientation, dynamic gait) and static balance (i.e. standing on two feet with eyes open, standing on two feet with eyes closed, etc.) to assess the risk of falling (Figure 9). The BBS consists of 14 balance-related items used in everyday life [43].Each item is graded from 0 to 4, with a maximum score of 56. To receive a full score for an item, an individual must be able to safely perform the item for (or within) a certain time allotment and without assistance.

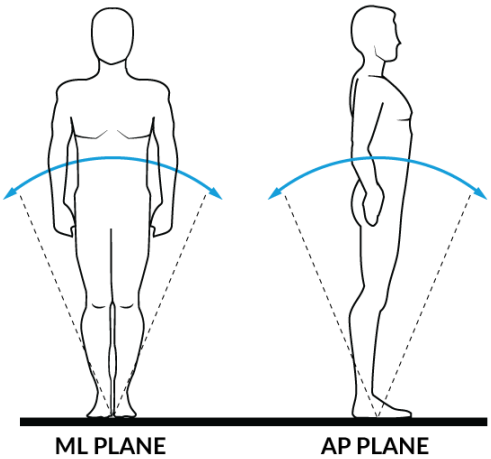

Figure 9. Planes of postural sway during the BBS.
ML = mediolateral; AP = anteroposterior.

A3.2 10 Meter Walk Test (10MWT)

The patient walks a twelve-meter distance in a straight line. A stopwatch is used to measure the time it takes to cover the central ten meters, allowing one meter before for acceleration and one meter after for deceleration (Figure 10). Three trials are collected at each of two walking conditions: a Self-Selected Velocity (SSV) and a Fast Velocity (FV), with an average time computed for each condition. To obtain the SSV and FV walking speed (outcome measure), the ten meters divided by the average time taken in seconds.

The importance of this test relies on the correlation between gait speed and ambulation ability. Increases in gait speed have been correlated with a higher quality of life [44].

The classification of patients by gait speed according to [23] is as follows:

1. < 0.4 m/s: household ambulators
2. 0.4 - 0.8 m/s: limited community ambulators
3. > 0.8 m/s: community ambulators

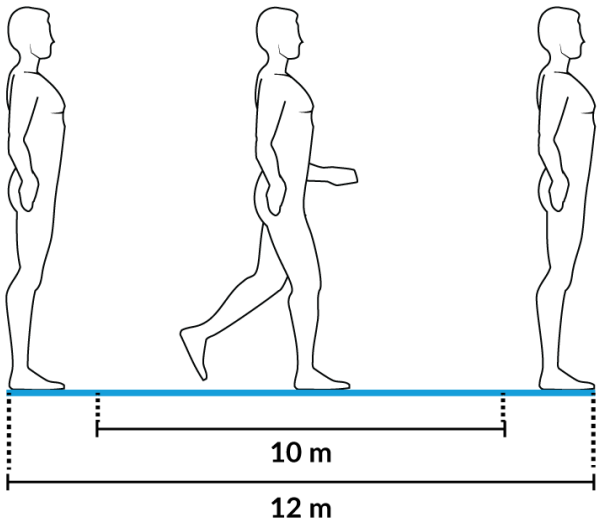

Figure 10. Representation of the 10MWT. Only the central 10 meters are recorded.

A3.3 Timed Up and Go (TUG)

The patient is seated in a chair with his/her back on the chair back. When the clinician says the “go” command, the patient walks a three-meter distance in a straight line, gives a 180 degree turn, comes back to the chair, turns a 180 degrees and sit. Timing begins from the go command and stops when the patient is finally seated (Figure 11).

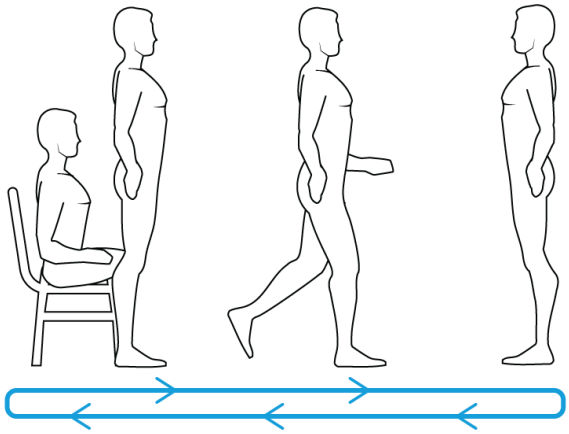

Figure 11. TUG clinical test consisting of six phases. 1. Sit-to-Stand, 2. Three-meter walk, 3. 180 deg turn, 4. Three-meter walk, 5. 108 deg turn, 6. Stand-to-Sit.

A3 Methods implemented to extract clinical outcome measures

This section describes the methods and algorithms to extract and estimate gait and balance features from the clinical outcome tests.

A3.1 Coordinate transformation method

An accelerometer measures a static vertical acceleration due to gravity besides the dynamic acceleration produced during walking. As [1] posits, whenever a reading deviates from the horizontal plane, the gravity component needs to be corrected by estimating only the dynamic acceleration due to the activity (i.e. walking) using the accelerometer's capacity as an inclinometer. This deviation is produced by the sensor placement location (L5), as it may be tilted due inaccurate placement in the participant's mediolateral plane or the lumbar curvature of the in the anteroposterior plane (Figure 12).

First, the measured acceleration signals (a_{AP}, a_{ML}, a_V) were transformed to a horizontal-vertical coordinate system proposed by [1]. The dynamic AP acceleration A_{AP} vector in the horizontal plane can be estimated by projecting the measured a_{AP}, and a_V in the horizontal plane by the following equation:

$$A_{AP} = a_{AP}cos\theta_a - a_v sin\theta_a$$

where θ_a is the angle between the horizontal plane and the A_{AP} in the sagittal plane with a positive direction being the forward acceleration. Then a provisional vertical acceleration vector A'_v needs to be estimated:

$$a'_v = a_{AP}sin\theta_a + cos\theta_a$$

Similarly to estimate the dynamic mediolateral acceleration vector A_{ML}, a projection of a_{ML} and the provisional acceleration vector a'_v:

$$A_{ML} = a_{ml}cos\theta_{ml} - a'_v sin\theta_{ml}$$

Finally to estimate the true vertical acceleration vector A_V:

$$A_V = a_{ml}sin\theta_{ml} + a'_v cos\theta_{ml} - 1g$$

Now to estimate the angles θ_{ml} and θ_{ap} [1] posits that the mean value of the measured acceleration along its sensitive axis will approach to the expected value for large *n*.

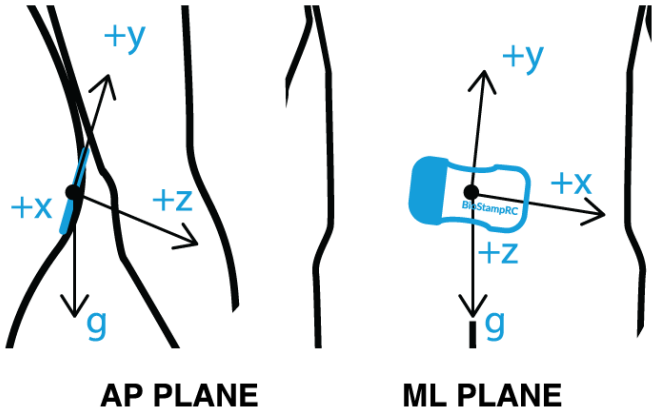

Figure 12. Sensor malignement. ML = mediolateral ; AP = anteroposterior.

A3.2 Continuous Wavelet Transform for gait event detection

The foot contact events (IC and EC) were estimated using the previously transformed vertical acceleration (A_V).This signal was filtered with a zero-lag second-order Butterworth filter at 10 Hz [4], using the MATLAB functions *detrend, butter* and *filtfilt*. A continuous wavelet transform method (CWT) is used to detect foot contact events, IC and EC [2]. This method decomposes the signal into time-spectral components [45-47], describing which frequencies are present at which times in the signal. This method transforms the signal at all scales and positions, maintaining the information without downsampling.

The CWT function of a signal $y(t)$ is defined as a convolution of this signal with a scaled and translated version of a mother wavelet Ψ [48]:

$$y(a,b) = \int_{-\infty}^{+\infty} y(t) \frac{1}{\sqrt{a}} \Psi^* \left(\frac{x - \bar{b}}{a} \right) dt$$

where a and b represent the scaling and translation factor respectively and Ψ^* represents the complex conjugate of the mother wavelet Ψ. The mother wavelet must fulfil the criteria of finite-energy and no zero-frequency components [46]. The scaling coefficients are inversely proportional to the spectral components, meaning that low scaling (high frequency components) provide more local information, whereas high scaling (low frequency components) provide more global information about the signal.

The method proposed by [2] uses the CWT with two wavelets, a Gaussian Wavelet and its derivative Mexican Hat Wavelet to detect IC and EC events, respectively (Figure 13). The scaling factor a of each wavelet is determined from [4] as:

$$a = \frac{F_c}{F_a \Delta}$$

where F_c is the center frequency of the wavelet (Hz), F_a is the most dominant frequency corresponding to the scale (obtained by the magnitude of power spectral density using the *fft* function in MATLAB), and Δ is the sampling period in seconds.

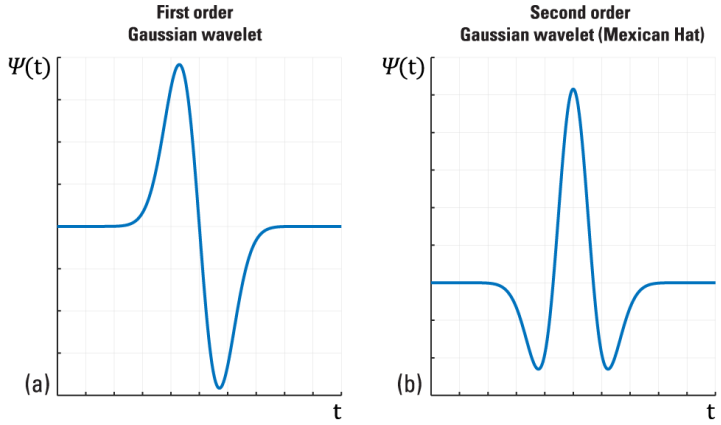

Figure 13. Wavelets proposed by [2] to estimate spatial gait features. (a). First order Gaussian to detect IC events. (b). Second order Gaussian (Mexican hat) to detect EC events.

First, the acceleration signal is integrated and then differentiated with the Gaussian Wavelet using its corresponding scaling factor $a1$ (with the MATLAB function *cwt* and *gaus1*), then the IC events were detected from the local minima of the applied CWT (*findpeaks* function). The signal is again differentiated using the Mexican Hat Wavelet and its corresponding previously derived scaling factor $a2$. The local maxima of the resulting signal corresponds to the EC events. Only peaks resulted from the maxima and minima with a magnitude >20% of the mean of all peaks were considered. To identify between right- and left-side ICs, the vertical angular velocity (yaw) was filter by a fourth order Butterworth filter at 2 Hz, and subsequently right and left were designated by directionality of the signal after zero-crossings (wherein the first step was left if the IC event occurred during negative filtered angular velocity, and right otherwise).

To remove false IC detections, ICs were constrained to be located within a time boundary from the previous IC (0.25-2.25 s) [5]. That is, the boundary ensured that local minima found too early or too late from the previous IC would not be counted as ICs. Finally, temporal features (*stride time*, *stance time* and *swing time*) were estimated by the relation of the foot events (IC and EC) to the double support phase of gait [3] (Figure 14).

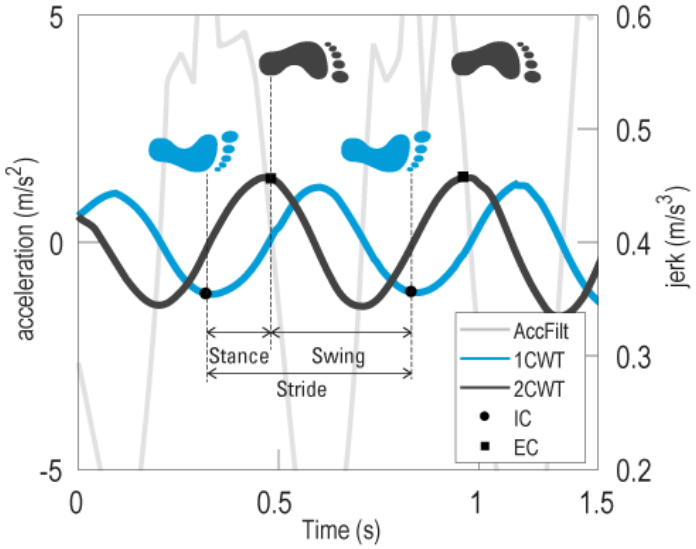

Figure 14. Gait event detection (IC, EC) [2], and temporal gait estimation of stride, stance and swing time proposed by [3] from the relation between the double support phase and the IC EC events. AccFilt = filtered acceleration; 1CWT = first cwt; 2CWT = second CWT; IC = initial contact; EC = end contact.

$$\text{Stance Time} = \text{EC(i} + 1) + \text{IC(i)}$$

$$\text{Stride Time} = \text{IC(i} + 2) - \text{IC(i)}$$

$$\text{Step Time} = \text{EC(i} + 1) - \text{IC(i)}$$

$$\text{Swing Time} = \text{Stride Time} - \text{Stance Time}$$

A3.3 Empirical Mode Decomposition

To estimate step length, the corrected vertical acceleration signal was first double integrated, resulting in vertical velocity and displacement of the CoM. It is important to note that integrating a time-series signal causes error to accumulates over time, which can drastically bias the estimated position. To eliminate this integration drift, the authors in [6] proposed the implementation of the *Empirical Decomposition Method* (*EDM*) developed by [28]. As a given signal (i.e. acceleration signal) is composed of both high and low frequency components, this method posits that the signal can be decomposed into a finite number of *Intrinsic Mode Functions* (*IMF*), wherein each IMF component is a decomposed waveform from the original signal ranging from high-frequency and low-frequency components (Figure 15).

This decomposition is based on the following assumptions: (1) the signal has at least two extrema (one minima and one maxima); (2) the time scale is defined by the time lapse between the extrema; and (3) if the data were totally devoid of extrema but contained only inflection points, then it can be differentiated once or more times to reveal the extrema [28].

From $x(t)$ the *EDM* can be summarized as follows:

1. Identify all the local minima and maxima of $x(t)$ (*findpeaks* function in MATLAB).
2. Compute the upper and lower envelopes based on the signal's from local maxima and minima, respectively, via interpolation with cubic spline, $env_{min}(t)$ and $env_{max}(t)$.
3. Compute the mean of the envelops, $m(t)$.

$$m(t) = \frac{env_{max} + \ env_{min}(t)}{2}$$

4. Subtract the mean $m(t)$ from the signal $x(t)$ to obtain the first component $d(t)$

$$d(t) = x(t) - m(t)$$

5. Treat $d(t)$ as the new data and iterate the previous steps (1-4) up to i times until $m_i(t)$ can be considered as a $zero - mean$. Thus, $d_i(t)$ becomes the first $IMF\ Im^{(1)}(t)$.

$$Im^{(1)}(t) = \ d_i(t) = \ d_{i(i-1)}(t) - m_i(t)$$

6. Define the residual $r_1(t) = x(t) - Im^{(1)}(t)$ as the new data and iterate on the previous steps until the last residual $r_k(t)$ contains one extrema.

From the all decompose $IMFs$ the original signal can be reconstructed as follows:

$$x(t) = \sum_{i=1}^{k} Im^{(i)}(t) + \ r_k(t)$$

The aforementioned method was applied both to the velocity and displacement data obtained from the integration of the vertical transformed acceleration signal A_V. In order to select the IMFs to reconstruct the signal without the baseline drift and based on prior visual check the Hurst exponent was implemented as it can serve as a measure of predictability of a time series [29]. Thus, IMFs with Hurst exponent values of < 0.8 were considered.

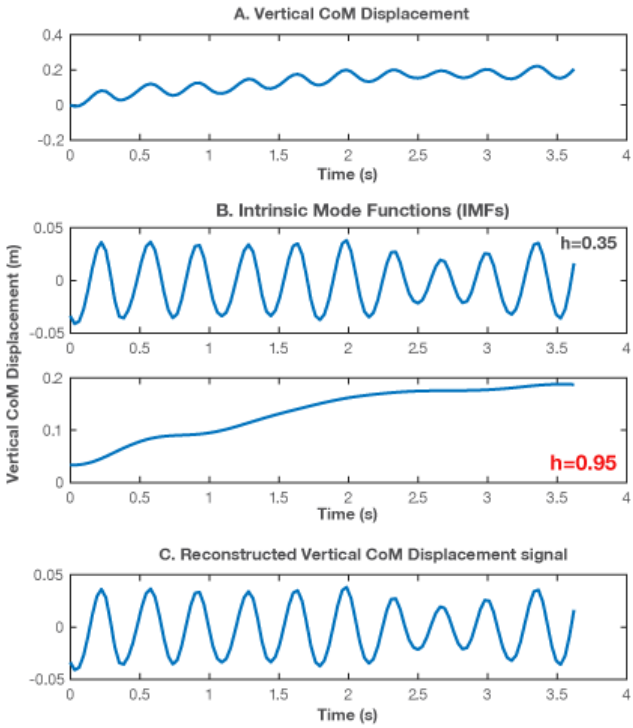

Figure 15. Empirical Mode Decomposition Method. A. Raw CoM displacement, B. Decomposed signal into Intrinsic Mode Functions (IMFs), D. Reconstructed signal from Hurst exponent values less than 0.8.

A3.4 Timed Up and Go phase detection by the discrete wavelet transform method (DWT)

The DWT method was used to de-noise the signal for detecting 3 phases: 1) rising from a chair (sit-to-stand), 2) turning, and 3) sitting down (stand-to sit) [31-33]. In the sit-to-stand phase, the trunk moves forward in preparation for standing producing a negative peak in the angular velocity about the x-axis (pitch) and a negative vertical acceleration peak; thereafter, the trunk moves backwards until it is in an upright position producing a positive angular velocity peak. This pattern is similar in the stand-to-sit transition but with a negative peak in the acceleration when the person sits. Therefore, these two acceleration peaks served as a starting point for the search windows of these two transition phases. Thus, the previously described CWT method (Appendix A3.2) was applied to the vertical acceleration signal (Figure 16).

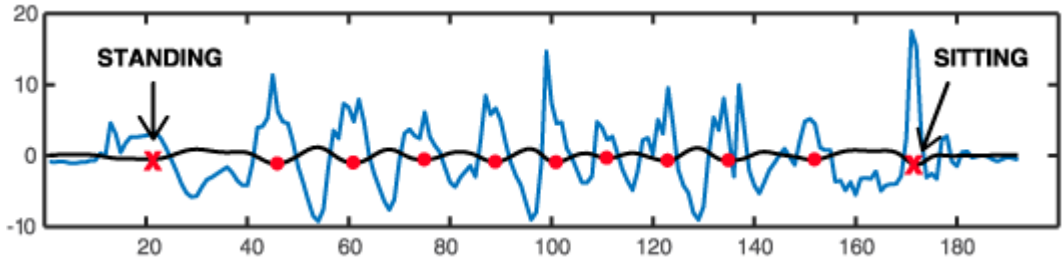

Figure 16. CWT method for step and stand/sit detections. The blue line represents the vertical acceleration signal, the black line the first derivative with the Gaussian wavelet, the dots the steps (ICs), and the “x” the sit/stand transitions.

Sit-to-Stand and Stand-to-Sit estimation

These phases were estimated by reconstruct the angular velocity signal around the x-axis (pitch) using a Daubechies mother wavelet (db5) with a level 2 approximation (2A) (Figure 17). After the signal was reconstructed, search windows were established (from 0% to 30% and from 80% to 100% of the length of the signal for the sit-to-stand and stand-to-sit phases, respectively) to isolate and improve the detection of each phase. To estimate the first peak (“ii” negative) a sub-search window was established (from 0 to 5% using as a reference the first IC event detected product of the participant standing, Figure 16). The beginning of the phase (i) was set as the first zero crossing before the negative peak (ii). The positive peak was determined as the maximum of the signal soon after the negative peak (ii).

Turning

To detect the turns while walking and before sitting down in a chair, the same db5 mother wavelet was applied to the yaw signal and reconstructed with a level 2 approximation (2A) (Figure 17). To isolate each turning phase, the first turn was estimated from 30% to 70% percent, and the second turn from 80% to 95% of the length of the signal. After this isolation, a local maximum was computed for each phase to determine the highest peak of the turn (i). Then, the zero crossing before and after the peak were used to estimate the start and end of the phase. Finally, to estimate the number of steps taken in each turn, the same search windows were used but on the previously computed CWT method (Figure 16).

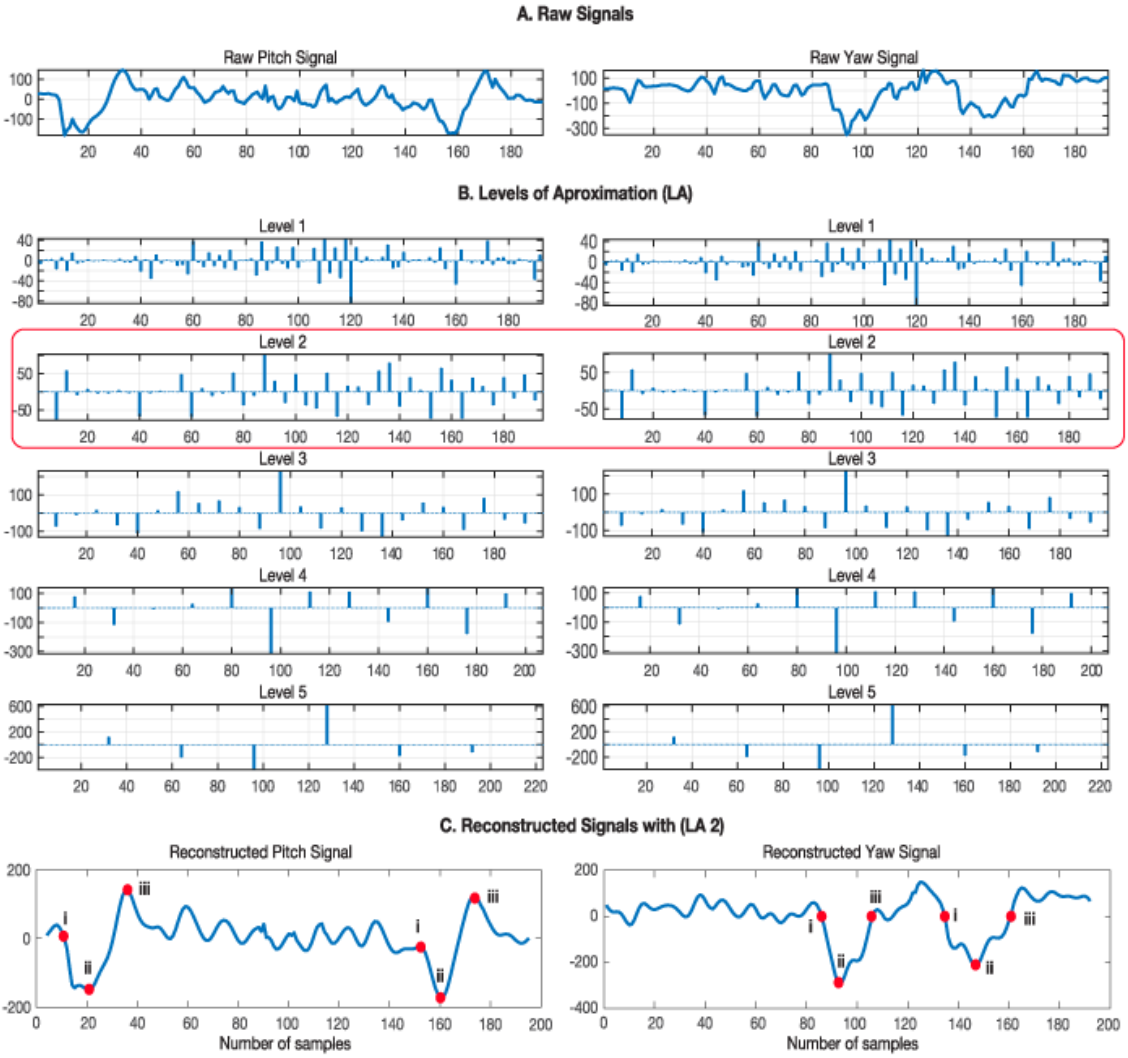

Figure 17. DWT method for the TUG phase identification. A. Raw angular velocity signals. B. Level of approximation and coefficients. C. Reconstructed signals.

A4 Tables of Results

Table 4. BBS standing with eyes closed. Features with simple and partial correlation coefficients controlling for weight and height (*) and normality significance values.

Features	Normality	All Participants (n =34)				By Gender			
						Women (n=20)		Men (n=14)	
	p	**r**	**p Value**	**r***	**p* Value**	**r***	**p* Value**	**r***	**p* Value**
F50% ML	.012	**-.373**	**.032***	**-.420**	**.019***	-.464	.052	-.317	.341
F50% AP	.001	-.106	.556	-.168	.366	-.187	.459	-.330	.321
F95% ML	.016	-.167	.352	-.183	.325	**-.513**	**.030***	.418	.201
F95% AP	**.483***	-.211	.240	-.206	.266	-.259	-.259	-.236	.485
SC AP	.034	-.144	.426	-.201	.278	-.217	.387	-.306	.359
SC ML	**.493***	**-.353**	**.044***	-.340	.062	**-.508**	**.031***	.034	.920
Max Acc AP	.000	.152	.399	.123	.510	.219	.382	-.290	.387
Max Acc ML	.000	.023	.900	.008	.964	.153	.545	-.477	.138
Mean Acc AP	.000	.129	.473	.146	.433	.230	.358	-.376	.254
Mean Acc ML	.000	.090	.617	.054	.772	.271	.276	-.410	.210
RMS AP	.000	.142	.431	.139	.457	.213	.395	-.342	.303
RMS ML	.000	.023	.899	.042	.822	.237	.343	-.453	.162
Ellipse Angles AP	.000	.021	.909	.081	.666	.250	.318	-.285	.395
Ellipse Angle ML	.000	-.068	.709	-.200	.282	-.194	.439	-.285	.395
Ellipse Area	.000	.011	.951	.079	.672	.162	.521	-.441	.174
Ellipse Axis AP	.000	.104	.563	.115	.536	.206	.411	-.408	.213
Ellipse Axis ML	.000	-.093	.608	.015	.936	.182	.471	-.479	.136
Jerk AP	.001	-.019	.918	.010	.956	.247	.323	-.460	.155
Jerk ML	.000	-.276	.119	-.134	.473	.013	.958	-.427	.190
SV AP	.000	.153	.394	.088	.638	.122	.629	-.384	.244
SV ML	.000	.177	.323	.091	.628	.383	.116	-.361	.275
SPathA AP	.001	-.019	.918	.010	.957	.247	.324	-.460	.154
SPathA ML	.000	-.276	.119	-.134	.473	.013	.958	-.427	.190

Notes: r* and p value*, partial correlation coefficients controlling for weight and height and its significance value.

Bolded results show significant p-values. * $p < 0.05$ for significant correlation and *$p > 0.05$ for normality distribution.

Features in italic were measured with Spearman, while the rest with Pearson correlation.

Table 5. BBS (standing with feet together). Features with simple and partial correlation coefficients controlling for weight and height (*) and normality significance values.

Features	Normality	All Participants (n = 34)				By Gender			
						Women (n=20)		Men (n=14)	
	p	**r**	**p Value**	**r***	**p* Value**	**r***	**p* Value**	**r***	**p* Value**
F50% ML	.000	-.144	.424	-.204	.271	-.425	.079	.549	.080
F50% AP	.008	-.052	.772	-.100	.592	-.138	.585	.090	.793
F95% ML	**.032***	-.212	.236	-.265	.149	**-.484**	**.042***	.283	.400
F95% AP	**.948***	-.060	.740	-.046	.806	-.324	.190	.416	.203
SC AP	**.111***	-.040	.826	-.023	.903	-.093	.713	.220	.515
SC ML	**.067***	-.251	.159	-.266	.148	**-.524**	**.026***	.446	.170
Max Acc AP	.000	**.383**	**.028***	**.422**	**.018***	**.662**	**.003***	.011	.974
Max Acc ML	.001	**.351**	**.045***	.318	.081	**.475**	**.046***	.114	.739
Mean Acc AP	.001	**.357**	**.042***	.342	.060	**.612**	**.007***	-.210	.535
Mean Acc ML	.002	**.351**	**.045***	.348	.055	**.556**	**.016***	-.098	.775
RMS AP	.005	**.380**	**.029***	**.405**	**.024***	**.666**	**.003***	-.144	.673
RMS ML	.000	**.393**	**.024***	.340	.061	**.547**	**.019***	-.043	.900
Ellipse Angles AP	.001	.035	.846	.011	.954	.323	.191	**-.606**	**.048***
Ellipse Angle ML	**.102***	-.022	.902	-.080	.670	-.238	.342	.233	.490
Ellipse Area	.002	**.426**	**.014***	**.383**	**.033***	**.610**	**.007****	.007	.984
Ellipse Axis AP	.017	**.429**	**.013***	**.401**	**.025***	**.672**	**.002****	-.052	.880
Ellipse Axis ML	.030	**.377**	**.031***	**.358**	**.048***	**.552**	**.018***	.277	.410
Jerk AP	**.090***	.192	.284	.267	.146	**.506**	**.032***	.256	.448
Jerk ML	.014	.174	.332	.129	.490	.126	.617	.532	.092
SV AP	.000	**.383**	**.028***	.337	.064	**.589**	**.010***	-.169	.619
SV ML	.000	**.349**	**.046***	**.357**	**.049***	**.640**	**.004****	-.440	.176
SPathA AP	**.092***	.192	.285	.267	.147	**.505**	**.032***	.256	.447
SPathA ML	.015	.174	.332	.128	.491	.126	.618	.532	.092

Notes: r* and p value*, partial correlation coefficients controlling for weight and height and its significance value. Bolded results show significant p-values. ** $p < 0.01$, * $p < 0.05$ for significant correlations and *$p > 0.05$ for normality distribution. Features in italic were measured with Spearman, while the rest with Pearson correlation.

Table 6. BBS (standing with one leg). Features with simple and partial correlation coefficients controlling for weight and height (*) and normality significance values.

Features	Normality	All Participants (n = 34)				By Gender			
						Women (n=20)		Men (n=14)	
	p	**r**	**p Value**	**r***	**p* Value**	**r***	**p* Value**	**r***	**p* Value**
F50% ML	.012	-.101	.574	-.095	.613	-.261	.296	.520	.101
F50% AP	.015	.224	.210	.198	.285	-.086	.734	.418	.200
F95% ML	.000	-.196	.273	-.150	.421	-.347	.159	.457	.158
F95% AP	.001	**.360**	**.040***	.325	.074	.170	.501	**.667**	**.025***
SC AP	**.486***	.265	.136	.263	.152	-.064	.800	**.673**	**.023***
SC ML	**.931***	-.102	.573	-.102	.584	-.318	.198	.602	.050
Max Acc AP	.000	.056	.755	.120	.519	.052	.837	.056	.871
Max Acc ML	.000	**.424**	**.014***	.345	.058	.259	.300	**.750**	**.008****
Mean Acc AP	.000	.042	.817	.015	.937	-.071	.780	-.181	.594
Mean Acc ML	.000	**.395**	**.023***	.311	.088	.325	.188	.377	.253
RMS AP	.000	.059	.743	.029	.876	-.048	.850	-.172	.614
RMS ML	.000	**.411**	**.017***	.315	.084	.312	.208	.436	.181
Ellipse Angles AP	.000	-.040	.827	.022	.908	.197	.433	-.107	.755
Ellipse Angle ML	.000	.027	.883	.132	.478	-.141	.576	.341	.304
Ellipse Area	.000	.177	.323	.136	.465	.090	.721	.263	.434
Ellipse Axis AP	.000	.220	.218	.185	.319	.095	.708	.336	.312
Ellipse Axis ML	.004	.107	.554	.118	.528	.083	.743	.209	.537
Jerk AP	**.138***	.185	.303	.189	.309	-.043	.867	**.632**	**.037***
Jerk ML	.000	.343	.050	.354	.051	.296	.234	**.669**	**.025***
SV AP	.000	.070	.698	.065	.730	.082	.747	-.413	.207
SV ML	.000	**.405**	**.019***	.307	.093	.385	.114	-.160	.639
SPathA AP	**.377***	.228	.201	.234	.205	.022	.932	**.633**	**.037***
SPathA ML	.000	**.359**	**.040***	**.363**	**.045***	.322	.192	**.669**	**.024***

Notes: r* and p value*, partial correlation coefficients controlling for weight and height and its significance value. Bolded results show significant p-values. ** $p < 0.01$, * $p < 0.05$ for significant correlations and *$p > 0.05$ for normality distribution. Features in italic were measured with Spearman, while the rest with Pearson correlation.

Table 7. BBS (standing unsupported). Features with simple and partial correlation coefficients controlling for weight and height (*) and normality significance values.

Features	Normality	All Participants				By Gender			
						Women (n=20)		Men (n=14)	
	p	**r**	**p Value**	**r***	**p* Value**	**r***	**p* Value**	**r***	**p* Value**
F50% ML	**0.082***	-.099	.585	-.118	.526	**-.559**	**.016***	**.630**	**.038***
F50% AP	**0.440***	-.220	.219	-.195	.293	-.312	.207	.054	.876
F95% ML	0.000	-.156	.385	-.107	.567	-.373	.127	.378	.252
F95% AP	**0.420***	.132	.465	.190	.305	.144	.568	.498	.119
SC AP	**0.440***	.055	.759	.102	.585	.065	.797	.356	.283
SC ML	**0.550***	-.071	.695	-.091	.626	**-.582**	**.011***	.602	.050
Max Acc AP	0.000	.061	.738	-.184	.322	**-.501**	**.034***	-.278	.407
Max Acc ML	0.000	-.168	.349	-.014	.939	-.257	.302	-.037	.913
Mean Acc AP	0.000	-.014	.937	-.155	.404	-.467	.051	-.380	.248
Mean Acc ML	0.000	-.167	.352	.012	.950	-.025	.920	-.563	.071
RMS AP	0.000	-.012	.949	-.162	.383	**-.474**	**.047***	-.357	.281
RMS ML	0.000	-.175	.330	-.002	.992	-.086	.734	-.493	.124
Ellipse Angles AP	0.000	-.067	.711	-.121	.516	-.079	.755	-.005	.988
Ellipse Angle ML	0.000	.043	.811	.066	.723	.123	.627	-.193	.570
Ellipse Area	0.000	-.127	.480	-.164	.377	**-.501**	**.034***	-.402	.221
Ellipse Axis AP	0.000	-.050	.782	-.161	.386	**-.478**	**.045***	-.379	.251
Ellipse Axis ML	0.012	-.213	.235	-.033	.862	-.103	.684	-.322	.334
Jerk AP	0.000	-.106	.556	-.176	.342	-.431	.074	-.233	.491
Jerk ML	0.022	-.182	.309	-.083	.657	-.218	.385	.022	.948
SV AP	0.000	-.021	.906	-.132	.479	-.420	.082	-.415	.205
SV ML	0.003	-.080	.660	-.031	.870	-.030	.905	-.516	.105
SPathA AP	0.000	-.109	.545	-.176	.342	-.431	.074	-.232	.492
SPathA ML	0.022	-.184	.305	-.083	.656	-.218	.384	.022	.948

Notes: r* and p value*, partial correlation coefficients controlling for weight and height and its significance value.

Bolded results show significant p-values. * $p < 0.05$ for significant correlation and *$p > 0.05$ for normality distribution.

Features in italic were measured with Spearman, while the rest with Pearson correlation.

Table 8. BBS (tandem standing). Features with simple and partial correlation coefficients controlling for weight and height (*) and normality significance values.

Features	Normality	All Participants (n=34)				By Gender			
						Women (n=20)		Men (n=14)	
	p	**r**	**p Value**	**r***	**p* Value**	**r**	**p Value**	**r***	**p* Value**
F50% ML	0.040	-.034	.850	-.051	.787	.202	.421	-.141	.679
F50% AP	0.000	.101	.578	.086	.645	.117	.645	.215	.526
F95% ML	**0.690***	-.045	.802	-.048	.797	.013	.959	.102	.765
F95% AP	0.000	-.327	.063	-.235	.203	-.222	.377	.054	.875
SC AP	**0.272***	-.174	.334	-.158	.395	-.185	.462	.185	.587
SC ML	**0.966***	-.093	.606	-.082	.663	.179	.476	-.051	.881
Max Acc AP	0.000	.316	.073	.162	.384	.214	.394	.070	.837
Max Acc ML	0.000	.218	.223	.080	.670	.023	.927	.276	.412
Mean Acc AP	0.007	**.424**	**.014***	**.369**	**.041***	.374	.126	.244	.470
Mean Acc ML	0.000	.242	.176	.137	.461	-.023	.928	.450	.165
RMS AP	0.003	**.422**	**.014***	.341	.060	.356	.147	.218	.520
RMS ML	0.000	.227	.205	.124	.507	-.002	.994	.410	.211
Ellipse Angles AP	0.000	.058	.750	.161	.388	.294	.237	-.287	.393
Ellipse Angle ML	0.046	**-.351**	**.045***	**-.423**	**.018***	**-.605**	**.008****	.216	.524
Ellipse Area	0.000	.241	.176	.139	.457	.071	.779	.333	.317
Ellipse Axis AP	0.001	.207	.248	.158	.395	.083	.744	.464	.151
Ellipse Axis ML	0.024	.291	.100	.203	.274	.169	.502	.313	.349
Jerk AP	**0.185***	.298	.092	.317	.083	.270	.278	.396	.228
Jerk ML	0.001	.091	.615	.140	.451	.133	.598	.463	.151
SV AP	0.000	.177	.323	.263	.153	.230	.359	.152	.656
SV ML	0.000	.233	.191	.110	.556	-.181	.473	.453	.161
SPathA AP	**0.187***	.298	.093	.316	.083	.270	.278	.396	.228
SPathA ML	0.001	.091	.615	.140	.451	.133	.599	.464	.151

Notes: r* and p value*, partial correlation coefficients controlling for weight and height and its significance value. Bolded results show significant p-values. ** $p < 0.01$, * $p < 0.05$ for significant correlations and *$p > 0.05$ for normality distribution. Features in italic were measured with Spearman, while the rest with Pearson correlation.

Table 9. 10MWT (SSV mode). Features with simple and partial correlation coefficients controlling for weight and height (*) and normality significance values.

Features	Normality	All Participants (n=33)				By Gender			
						Women (n=19)		Men (n=14)	
	p	**r**	**p Value**	**r***	**p* Value**	**r***	**p* Value**	**r***	**p* Value**
Vertical Displacement	0.000	-.155	.388	-.111	.552	**-.518**	**.033***	.219	.493
Mean Stance Time	**0.722***	-.010	.957	.117	.531	**.520**	**.032***	-.292	.357
Mean Step Time	**0.661***	-.052	.775	.068	.714	**.571**	**.017***	-.435	.158
Mean Stride	**0.672***	-.061	.737	.058	.758	**.554**	**.021***	-.434	.159
Mean Swing Time	**0.413***	-.121	.502	-.024	.896	**.551**	**.022***	**-.580**	**.048***
Mean Step Length	0.013	-.078	.668	-.109	.558	-.481	.051	.059	.855
Maximum Power Frequency	0.001	-.148	.413	-.185	.320	**-.561**	**.019***	.272	.392
Stance Time Symmetry Ratio	**0.625***	-.104	.564	-.083	.656	-.173	.506	-.101	.755
Step Length Symmetry Ratio	0.029	.307	.083	.284	.121	.012	.963	.539	.070
Duration	**0.925***	.047	.794	.078	.678	**.566**	**.018***	-.344	.273
Mean Velocity	**0.407***	-.087	.632	-.153	.410	**-.618**	**.008****	.282	.375
N Steps	**0.311***	.099	.584	.024	.900	.454	.067	-.302	.339

Notes: r* and p value*, partial correlation coefficients controlling for weight and height and its significance value.

Bolded results show significant p-values. ** $p < 0.01$, * $p < 0.05$ for significant correlations and *$p > 0.05$ for normality distribution. Features in italic were measured with Spearman, while the rest with Pearson correlation.

Table 10. 10MWT (FV mode). Features with simple and partial correlation coefficients controlling for weight and height (*) and normality significance values.

Features	Normality	All Participants (n=32)				By Gender			
						Women (n=18)		Men (n=14)	
	p	**r**	**p Value**	**r***	**p* Value**	**r***	**p* Value**	**r***	**p* Value**
Vertical Displacement	**0.503***	**-.396**	**.025***	**-.377**	**.040***	**-.560**	**.024***	-.181	.573
Mean Stance Time	**0.323***	-.232	.202	-.185	.329	.019	.945	-.291	.359
Mean Step Time	**0.255***	-.244	.179	-.202	.284	-.014	.960	-.278	.382
Mean Stride	**0.252***	-.241	.183	-.199	.293	-.004	.989	-.278	.382
Mean Swing Time	**0.191***	-.239	.187	-.201	.287	-.042	.877	-.234	.464
Mean Step Length	**0.983***	-.345	.053	-.323	.081	**-.522**	**.038***	-.273	.391
Maximum Power Frequency	0.018	-.292	.105	-.356	.054	**-.587**	**-.017***	-.092	.776
Stance Time Symmetry Ratio	**0.635***	-.143	.435	-.125	.511	.000	1.000	-.391	.209
Step Length Symmetry Ratio	**0.701***	.160	.382	.210	.265	.059	.828	.344	.274
Duration	**0.439***	.092	.617	.085	.655	.276	.301	-.016	.961
Mean Velocity	**0.265***	-.008	.964	-.068	.722	-.380	.147	.089	.784
N Steps	**0.888***	.347	.052	.319	.086	.337	.202	.387	.214

Notes: r* and p value*, partial correlation coefficients controlling for weight and height and its significance value.

Bolded results show significant p-values. * $p < 0.05$ for significant correlation and *$p > 0.05$ for normality distribution.

Features in italic were measured with Spearman, while the rest with Pearson correlation.

Table 11. TUG. Features with simple and partial correlation coefficients controlling for weight and height (*) and normality significance values.

	Features	Normality	All Participants (n=32)				By Gender			
							Women (n=19)		Men (n=13)	
		p	**r**	**p Value**	**r***	**p* Value**	**r***	**p* Value**	**r***	**p* Value**
Sit-to-Stand	Range Pitch (i-ii)	**0.560***	**-.369**	**.038***	**-.384**	**.036***	**-.574**	**.016***	-.043	.901
	Range Pitch (ii-iii)	**0.383***	-.266	.141	-.266	.155	-.475	.054	-.011	.974
	STD Pitch (i-iii)	**0.149***	-.343	.055	-.340	.066	**-.613**	**.009****	-.032	.925
	Mean Pitch (i-iii)	**0.229***	**.426**	**.015***	**.410**	**.024***	**.651**	**.005****	.215	.525
	Median Pitch (i-iii)	**0.330***	.284	.116	.258	.168	.393	.119	.255	.449
	Mag Pitch (i-ii)	**0.694***	**.349**	**.050***	.359	.051	**.574**	**.016***	.021	.952
	Mag Pitch (ii-iii)	**0.056***	.054	.769	.067	.726	-.058	.826	.027	.938
	Slope Pitch (i-ii)	0.000	**.356**	**.046***	**.383**	**.037***	**.592**	**.012***	.248	.463
	Slope Pitch (ii-iii)	**0.069***	-.263	.146	-.258	.168	**-.567**	**.018***	.023	.947
	Mean Acc AP (i-iii)	**0.937***	**-.370**	**.037***	**-.378**	**.040***	-.384	.128	-.360	.277
	STD Acc AP (i-iii)	**0.248***	-.221	.225	-.186	.325	-.249	.334	-.119	.728
	Duration (i-iii)	**0.387***	.329	.066	.312	.093	**.531**	**.028***	.120	.726
	Median Acc AP (i-iii)	**0.523***	-.104	.573	-.170	.370	-.170	.513	-.122	.720
Stand-to-Sit	Range Pitch (i-ii)	**0.236***	**-.355**	**.046***	**-.392**	**.032***	**-.484**	**.049***	-.296	.376
	Range Pitch (ii-iii)	**0.949***	-.250	.167	-.285	.127	-.341	.181	-.151	.657
	STD Pitch (i-iii)	**0.376***	-.240	.186	-.282	.131	-.376	.136	-.059	.863
	Mean Pitch (i-iii)	**0.649***	.014	.937	.004	.983	.134	.607	.091	.789
	Median Pitch (i-iii)	**0.457***	-.068	.713	-.093	.624	-.092	.725	.035	.919
	Mag Pitch (i-ii)	**0.079***	.310	.084	.337	.068	**.524**	**.031***	.186	.584
	Mag Pitch (ii-iii)	**0.877***	-.152	.406	-.174	.357	-.102	.696	-.106	.757
	Slope Pitch (i-ii)	0.044	.308	.086	.271	.147	.423	.091	.012	.973
	Slope Pitch (ii-iii)	**0.055***	**-.370**	**.037***	**-.445**	**.014***	**-.502**	**.040***	-.296	.376
	Mean Acc AP (i-iii)	**0.801***	-.221	.224	-.270	.148	-.422	.092	.091	.790
	STD Acc AP (i-iii)	**0.108***	-.279	.122	-.301	.107	-.354	.163	-.179	.598
	Duration (i-iii)	**0.626***	.308	.086	.351	.057	**.519**	**.033***	-.098	.774
	Median Acc AP (i-iii)	**0.459***	-.039	.831	-.071	.710	-.181	.487	.202	.552
Turn 1	Duration	**0.067***	.087	.634	.130	.493	.228	.378	.075	.827
	N Steps	**0.481***	-.106	.565	-.088	.642	.029	.912	-.057	.868
	Mag Yaw	**0.753***	-.139	.447	-.124	.515	-.299	.244	.141	.680
	Slope Yaw (i-ii)	0.000	-.175	.339	-.087	.647	-.465	.060	.350	.292
	Slope Yaw (ii-iii)	0.000	.263	.146	.211	.263	.099	.704	.436	.180
Turn 2	Duration	**0.087***	.288	.110	.344	.063	.454	.067	.106	.757
	N Steps	**0.648***	.277	.125	.260	.166	.250	.333	.198	.559
	Mag Yaw	**0.462***	**-.361**	**.042***	**-.369**	**.045***	**-.501**	**.041***	-.082	.811
	Slope Yaw (i-ii)	0.012	**-.545**	**.001****	**-.538**	**.002****	**-.652**	**.005****	-.285	.395
	Slope Yaw (ii-iii)	**0.265***	.213	.242	.225	.231	.291	.257	.031	.928
Walk	RMS Acc AP	**0.576***	**.451**	**.001****	**.455**	**.012***	**.571**	**.017***	.193	.569
	RMS Acc ML	**0.214***	.085	.643	.097	.612	.321	.209	.006	.987
	RMS Acc V	**0.121***	.249	.170	.247	.188	.150	.566	.339	.308
	N Steps	**0.468***	**.356**	**.046***	.355	.054	.447	.072	.162	.635

Mean Step Time	**0.802***	-.001	.996	.046	.810	.076	.773	-.080	.815
STD Step Time	**0.701***	.077	.674	.178	.346	.348	.171	.092	.788

Notes: r* and p value*, partial correlation coefficients controlling for weight and height and its significance value.

Bolded results show significant p-values. ** p < 0.01, * p < 0.05 for significant correlations and *p > 0.05 for normality distribution. Features in italic were measured with Spearman, while the rest with Pearson correlation.

Table 12. Velocity difference from the 10MWT (SSV & FV modes). Features with simple and partial correlation coefficients controlling for weight and height (*) and normality significance values.

Features	Normality	All Participants				By Gender			
						Women (n=19)		Men (n=14)	
	p	**r**	**p Value**	**r***	**p* Value**	**r***	**p* Value**	**r***	**p* Value**
Velocity Diff (FV-SSV)	**0.674***	.124	.499	.126	.507	.340	.197	-.320	.311

Notes: r* and p value*, partial correlation coefficients controlling for weight and height and its significance value.

Bolded results show significant p-values. * p < 0.05 for significant correlation and *p > 0.05 for normality distribution.

Features in italic were measured with Spearman, while the rest with Pearson correlation.

Bibliography

1. Moe-Nilssen, R., *A new method for evaluating motor control in gait under real-life environmental conditions. Part 1: The instrument.* Clinical Biomechanics, 1998. **13**(4): p. 320-327.
2. McCamley, J., et al., *An enhanced estimate of initial contact and final contact instants of time using lower trunk inertial sensor data.* Gait Posture, 2012. **36**(2): p. 316-8.
3. Din, S.D., A. Godfrey, and L. Rochester, *Validation of an Accelerometer to Quantify a Comprehensive Battery of Gait Characteristics in Healthy Older Adults and Parkinson's Disease: Toward Clinical and at Home Use.* IEEE Journal of Biomedical and Health Informatics, 2016. **20**(3): p. 838-847.
4. Pham, M.H., et al., *Validation of a Step Detection Algorithm during Straight Walking and Turning in Patients with Parkinson's Disease and Older Adults Using an Inertial Measurement Unit at the Lower Back.* Frontiers in Neurology, 2017. **8**: p. 457.
5. Najafi, B., et al., *Ambulatory system for human motion analysis using a kinematic sensor: monitoring of daily physical activity in the elderly.* IEEE Transactions on Biomedical Engineering, 2003. **50**(6): p. 711-723.
6. Qi, Z., et al., *Improved method of step length estimation based on inverted pendulum model.* International Journal of Distributed Sensor Networks, 2017. **13**(4): p. 1550147717702914.
7. Benjamin, E.J., et al., *Heart Disease and Stroke Statistics-2017 Update: A Report From the American Heart Association.* Circulation, 2017. **135**(10): p. e146-e603.
8. Stevens, E.G.V., et al., *The burden of stroke in Europe*. 2017. 108-108.
9. Schmidt, H., et al., *Gait rehabilitation machines based on programmable footplates.* J Neuroeng Rehabil, 2007. **4**(1): p. 2.
10. Kwakkel, G., B.J. Kollen, and R.C. Wagenaar, *Therapy Impact on Functional Recovery in Stroke Rehabilitation.* Physiotherapy, 1999. **85**(7): p. 377-391.
11. Dobkin, B.H., *Clinical practice. Rehabilitation after stroke.* N Engl J Med, 2005. **352**(16): p. 1677-84.
12. Ruth, D., *Rehabilitation of Gait Speed After Stroke: A Critical Review of Intervention Approaches.* Neurorehabilitation and Neural Repair, 2008. **22**(6): p. 649-660.
13. Knecht, S., S. Hesse, and P. Oster, *Rehabilitation after stroke.* Dtsch Arztebl Int, 2011. **108**(36): p. 600-6.
14. Barker, S., et al., *Accuracy, reliability, and validity of a spatiotemporal gait analysis system.* Med Eng Phys, 2006. **28**(5): p. 460-7.
15. Chen, S., et al., *Toward Pervasive Gait Analysis With Wearable Sensors: A Systematic Review.* IEEE J Biomed Health Inform, 2016. **20**(6): p. 1521-1537.
16. Lonini, L., et al., *Automatic detection of spasticity from flexible wearable sensors*, in *Proceedings of the 2017 ACM International Joint Conference on Pervasive and Ubiquitous Computing and Proceedings of the 2017 ACM International Symposium on Wearable Computers*. 2017, ACM: Maui, Hawaii. p. 133-136.
17. Moon, Y., et al., *Monitoring gait in multiple sclerosis with novel wearable motion sensors.* PLoS One, 2017. **12**(2): p. e0171346.
18. Sun, R., et al., *Assessment of Postural Sway in Individuals with Multiple Sclerosis Using a Novel Wearable Inertial Sensor.* Digital Biomarkers, 2018. **2**(1): p. 1-10.
19. Mancini, M., et al., *ISway: a sensitive, valid and reliable measure of postural control.* Journal of NeuroEngineering and Rehabilitation, 2012. **9**(1): p. 59.
20. Perry, J. and J.M. Burnfield, *Gait Analysis: Normal and Pathological Function, Second Edition.* Gait Analysis: Normal and Pathological Function, Second Edition, 2010. **9**(2): p. 1-551.
21. Lajoie, Y. and S.P. Gallagher, *Predicting falls within the elderly community: comparison of postural sway, reaction time, the Berg balance scale and the Activities-specific Balance Confidence (ABC) scale for comparing fallers and non-fallers.* Archives of Gerontology and Geriatrics, 2004. **38**(1): p. 11-26.
22. Park, J.-H., et al., *Quantifying effects of age on balance and gait with inertial sensors in community-dwelling healthy adults.* Experimental Gerontology, 2016. **85**: p. 48-58.
23. Bowden, M.G., et al., *Validation of a speed-based classification system using quantitative measures of walking performance poststroke.* Neurorehabil Neural Repair, 2008. **22**(6): p. 672-5.

24. Shumway-Cook, A., S. Brauer, and M. Woollacott, *Predicting the Probability for Falls in Community-Dwelling Older Adults Using the Timed Up & Go Test.* Physical Therapy, 2000. **80**(9): p. 896-903.
25. Palmerini, L., et al., *Feature selection for accelerometer-based posture analysis in Parkinson's disease.* IEEE Trans Inf Technol Biomed, 2011. **15**(3): p. 481-90.
26. Vervoort, D., et al., *Multivariate analyses and classification of inertial sensor data to identify aging effects on the timed-Up-and-Go test.* PLoS ONE, 2016. **11**(6): p. 1-17.
27. Zijlstra, W. and A.L. Hof, *Assessment of spatio-temporal gait parameters from trunk accelerations during human walking.* Gait Posture, 2003. **18**(2): p. 1-10.
28. Huang, N.E., et al., *The empirical mode decomposition and the Hilbert spectrum for nonlinear and non-stationary time series analysis.* Proceedings of the Royal Society of London. Series A: Mathematical, Physical and Engineering Sciences, 1998. **454**(1971): p. 903.
29. Namazi, H., et al., *A signal processing based analysis and prediction of seizure onset in patients with epilepsy.* Oncotarget, 2016. **7**(1): p. 342-350.
30. Schubert, P. and M. Kirchner, *Ellipse area calculations and their applicability in posturography.* Gait & Posture, 2014. **39**(1): p. 518-522.
31. Vervoort, D., et al., *Multivariate Analyses and Classification of Inertial Sensor Data to Identify Aging Effects on the Timed-Up-and-Go Test.* PLoS One, 2016. **11**(6): p. e0155984.
32. Weiss, A., et al., *Using a Body-Fixed Sensor to Identify Subclinical Gait Difficulties in Older Adults with IADL Disability: Maximizing the Output of the Timed Up and Go.* PLOS ONE, 2013. **8**(7): p. e68885.
33. Weiss, A., et al., *An instrumented timed up and go: the added value of an accelerometer for identifying fall risk in idiopathic fallers.* Physiological Measurement, 2011. **32**(12): p. 2003.
34. Chiari, L., L. Rocchi, and A. Cappello, *Stabilometric parameters are affected by anthropometry and foot placement.* Clinical Biomechanics, 2002. **17**(9): p. 666-677.
35. Lee, C.R. and C.T. Farley, *Determinants of the center of mass trajectory in human walking and running.* The Journal of Experimental Biology, 1998. **201**(21): p. 2935.
36. Lord, S., R. D Clark, and I. Webster, *Postural Stability and Associated Physiological Factors in a Population of Aged Persons*. Vol. 46. 1991. M69-76.
37. JudgeRoy, J.O., I.B. Davis, and S. Õunpuu, *Step Length Reductions in Advanced Age: The Role of Ankle and Hip Kinetics.* The Journals of Gerontology: Series A, 1996. **51A**(6): p. M303-M312.
38. Greve, C., et al., *Not All Is Lost: Old Adults Retain Flexibility in Motor Behaviour during Sit-to-Stand.* PLOS ONE, 2013. **8**(10): p. e77760.
39. Riley, P.O., et al., *Mechanics of a constrained chair-rise.* Journal of Biomechanics, 1991. **24**(1): p. 77-85.
40. Lummel, R.V., *Assessing Sit-to-Stand for Clinical Use.* 2017: p. 194-194.
41. Cavagna, G.A. and R. Margaria, *Mechanics of walking.* J Appl Physiol, 1966. **21**(1): p. 271-8.
42. AbilityLab, S.R., *Rehabilitation Measures Database.* 2018.
43. Berg, K., *Measuring balance in the elderly: Preliminary development of an instrument*. Vol. 41. 1989. 304-311.
44. Perry, J., et al., *Classification of walking handicap in the stroke population.* Stroke, 1995. **26**(6): p. 982-9.
45. Torrence, C. and G.P. Compo, *A practical guide to wavelet analysis.* Bulletin of the American Meteorological Society, 1998. **79**(1): p. 61-78.
46. Addison, P., J. Walker, and R. Guido, *Time--frequency analysis of biosignals.* IEEE Eng Med Biol Mag, 2009. **28**(5): p. 14-29.
47. Khandelwal, S. and N. Wickström, *Gait Event Detection in Real-World Environment for Long-Term Applications: Incorporating Domain Knowledge Into Time-Frequency Analysis.* IEEE Transactions on Neural Systems and Rehabilitation Engineering, 2016. **24**(12): p. 1363-1372.
48. Khandelwal, S. and N. Wickstrom, *Novel methodology for estimating Initial Contact events from accelerometers positioned at different body locations.* Gait Posture, 2018. **59**: p. 278-285.